Nationaal Lucht- en Ruimtevaartlaboratorium
National Aerospace Laboratory NLR

NLR-TP-2000-302

Propagation lifetime calculation of the P&W compressor fan disc

Life prediction based on crack growth

O. Kogenhop

Nationaal Lucht- en Ruimtevaartlaboratorium
National Aerospace Laboratory NLR

NLR-TP-2000-302

Propagation lifetime calculation of the P&W compressor fan disc

Life prediction based on crack growth

O. Kogenhop

This investigation has been carried out as a Master's thesis for the Delft University of Technology, faculty Mechanical Engineering and Marine Engineering, section Process and Energy with main subject Gas Turbines. The investigation has been carried out under supervision of prof. ir. J.P. van Buijtenen and ir. T. Tinga.

Division: Structures and Materials
Issued: 31 May 2000
Classification of title: Unclassified

Summary

The main object of this report is to investigate whether it is possible to determine the propagation lifetime for complicated gas turbine components by performing crack growth calculations. Therefore a certain calculation course/strategy is necessary, which will be shown in this report. As a case study the present 2^{nd}-stage fan disc of a Pratt & Whitney engine of the RNLAF F16 is used. This fan disc is part of a three-stage rotor fan, and provides the transmission of the loads through an attached hub to the outer (low-pressure) shaft. This disc has been known to show cracks that develop from the thrust balance holes in the hub.

The key elements in the strategy are: investigation of the load spectrum, determination of the load sequence, investigation of the materials' crack growth properties, determination of the stress intensity factor solution, and the determination of a start- and stop criterion. The loads on the 2^{nd}-stage fan disc are investigated. The main loads are the loads due to torsion and due to the axial force of the blades. In this investigation the torsion loads are determined with the use of a dynamic gas turbine program, GSP. Real mission data from the RNLAF is used as input for GSP. A random generator program is used to create a load sequence file from this data, where the diversification of missions the RNLAF flies and the mission mix are taken into account. A damage tolerance materials handbook is used to provide the necessary crack growth data for the crack growth rate relation, which is a function that describes the crack growth behaviour. The stress intensity factor solution is determined with the use of finite elements, because the geometry of the 2^{nd}-stage fan disc is too complex to be described by infinite plate solutions. Finally an effort is taken to determine the present stop criterion. As start criterion the initial crack size Pratt & Whitney uses is used. These aspects are implemented in a crack growth calculation program, which determines the propagation lifetime.

The results of the propagation lifetime calculations using the critical crack sizes from Pratt & Whitney look promising. Same lifetimes are obtained for the larger critical crack sizes.

The results also show that the crack growth relation plays a significant role in the lifetime calculation. The fit constants obtained with the fit of the crack growth data seem to have large inaccuracies, which effects the lifetime calculation. The main conclusion of this report is that actual life predictions, for other components, can be performed when accurate material data, load sequence, stress intensity factor solution, and initial and critical crack lengths are known. This report shows that with the current data a reasonable lifetime estimation can be made, even when not all of the data is accurate. Another conclusion is that in determining the stress intensity factor solution, finite element methods are usefull tools, and produce stress intensity factor solutions for complex geometries.

Samenvatting

Het belangrijkste doel van dit rapport is het onderzoeken of het mogelijk is om voor gecompliceerde gasturbinecomponenten scheurgroeisommen te maken. Hiervoor is een bepaalde oplosstrategie nodig, welke in dit rapport zal worden behandeld. Als studieobject zal de tweedetraps fandisk uit de Pratt & Whitney gasturbine van de F-16 van de Koninklijke Luchtmacht worden gebruikt. De fandisk is een onderdeel van een drietraps rotorfanmodule, en zorgt voor het overbrengen van belastingen door de aangehechte naaf (hub) naar de lagedrukas. Van de disk is bekend dat er na verloop van tijd scheuren ontwikkelen en groeien van de thrust balance holes in de richting van de naaf.

De belangrijkste onderdelen van de oplosstrategie zijn het onderzoeken van het belastingspectrum, de bepaling van de belastingvolgorde, het onderzoeken van het scheurgroeigedrag van het materiaal, de bepaling van de spanningsintensiteitsfactor, en de bepaling van een start- en een stopcriterium. De belastingen op de 2^{de}-traps fandisk worden onderzocht. De belangrijkste belastingen zijn de belasting ten gevolge van torsie en de belasting ten gevolge van de axiale trekkracht op de schoepen. In dit onderzoek wordt de torsiebelasting bepaald door gebruik te maken van een dynamisch gasturbine-rekenprogramma, GSP. Actuele missiedata van de Koninklijke Luchtmacht wordt gebruikt als input voor GSP. Hiermee wordt met gebruik van een C++ programma een willekeurige belastingsvolgorde gegenereerd, waarbij rekening gehouden wordt met de verscheidenheid van missies en de missie-mix. Om het scheurgroeigedrag van het diskmateriaal te beschrijven wordt data uit een ”damage tolerant”-materiaalhandboek gebruikt. De spanningsintensiteitsoplossing wordt bepaald door gebruik te maken van een eindige-elementenmodel omdat de 2^{de}-traps fandisk te complex is om de oplossing te bepalen met gebruik van oneindigeplaatoplossingen. Als laatste is er gezocht naar een criterium waardoor de scheurgroeiberekening zou moeten worden gestopt. Deze aspecten worden in een scheurgroei programma geïmplementeerd waarmee de propagatielevensduur wordt bepaald.

De resultaten van de scheurgroeiberekening ogen hoopvol als er gebruik wordt gemaakt van kritische scheurlengtes die Pratt & Whitney gebruikt. Voor de grotere scheurlengtes kunnen soortgelijke levensduren worden verkregen.

Uit de resultaten blijkt dat de beschrijving van het materiaalgedrag een belangrijke rol speelt in de levensduurbepaling. De fitconstanten in de scheurgroeirelatie blijken onnauwkeurig te zijn, waardoor de levensduurbepaling onnauwkeuriger wordt. De belangrijkste conclusie van dit rapport is dat levensduurvoorspellingen op basis van scheurgroei inderdaad gemaakt kunnen worden, mits er voldoende (juiste) data bekend is van het materiaal, de belastingvolgorde, spanningsintensiteitsoplossing en de kritieke en initiële scheurlengtes. Dit rapport toont aan dat met de huidige data, welke niet in alle gevallen volledig bekend is, soortgelijke levensduurvoorspellingen gemaakt kunnen worden.

Een belangrijk hulpmiddel hierin is de bepaling van spanningsintensiteitsoplossingen voor complexe componenten met behulp van eindige elementen.

Contents

(94 pages in total)

List of Symbols, Constants, Indices, and Abbreviations

Symbols

a	$[mm]$	crack length
a_0	$[mm]$	intrinsic crack length
a, b	$[mm]$	width, height
f	$[-]$	crack opening function
h	$[mm]$	height
n	$[n]$	normal
P	$[N]$	force
r	$[mm]$	radius
u, v, w	$[mm]$	displacement components
x, y, z	$[mm]$	coordinates
A_0, A_1, A_2, A_3	$[-]$	coefficients in crack opening function
D	$[mm]$	diameter
E	$[MPa]$	Young's modulus
G	$[MPa]$	shear modulus
J	$[mm^4]$	polar moment of inertia
K	$[MPa\sqrt{mm}]$	stress intensity factor
K_t	$[-]$	stress concentration factor
N	$[-]$	amount of cycles
N_{cr}	$[-]$	number of cycles at critical crack size
N_D	$[-]$	amount of cycles at design life (aircraft)
R	$[-]$	stress ratio
S	$[MPa]$	stress
T	$[Nm]$	torque
U	$[-]$	calculation factor
$\frac{da}{dN}$	$[mm/cycle]$	rate of crack growth
$\frac{S_{max}}{\sigma_0}$	$[-]$	ratio of max applied stress to the flow stress
α	$[-]$	constraint factor
ϕ	$[rad]$	angle of twist
ϕ_i	$[-]$	geometric parameter

σ	$[MPa]$	direct stress
τ	$[MPa]$	shear stress
ν	$[-]$	Poisson's ratio
ρ	$[mm]$	radius of curvature
Δa	$[mm]$	amount of crack growth
ΔN	$[-]$	amount of fatigue cycles
ΔK	$[MPa\sqrt{mm}]$	difference between K_{max} and K_{min}

Constants

C, n, p, q	$[-]$	constants for the crack growth equation
a, b, c, d, e, f	$[-]$	fit parameters for the crack growth equation

Indices

c, cr	critical
eff	effective
i	initial, or summation mark
th	threshold
max	maximum
min	minimum
x, y, z	direction of plane normals on which stresses work
xy, xz, yz	in the context of stresses the first subscript gives the plane normal direction, the second subscript gives stress direction (example: τ_{xy} is the shear stress acting on plane which has a normal in x-direction, in the positive y-direction)

Abbreviations

CCY	Calculated CYcles
CFD	Computational Fluid Dynamics
CRAGRO	NLR's modular crack growth program
ESA	European Space Agency
FACE	Fatigue Analyser & Autonomous Combat Evaluation

FE	Finite Element
FEM	Finite Element Method
GSP	Gas turbine Simulation Program
HCF	High Cycle Fatigue
IFM	Inlet Fan Module
LCF	Low Cycle Fatigue
LEFM	Linear Elastic Fracture Mechanics
LP	Low Pressure
NASA	National Aeronautics and Space Administration
NASGRO	NASA's crack growth program
NASTRAN	product name of the MacNeal-Schwendler corporation
NLR	National Aerospace Laboratory
PATRAN	product name of the MacNeal-Schwendler corporation
PW	Pratt & Whitney
PWA	Pratt & Whitney Aircraft
RNLAF	Royal Netherlands Air Force
TAC	Total Accumulated Cycles
USAF	United States Air Force

This page is intentionally left blank

1 Introduction

1.1 Background

For the economical use of gas turbines it is important to determine the actual service life of gas turbine components that are subjected to operational conditions. These days, repair and maintenance intervals are either determined by engine manufacturers or derived from maintenace intervals of other users or airforce bases. Engine manufacturers frequently base their calculations on heavy use, so that a conservative lifetime is obtained. Most parts will be loaded less severe, and will thus be replaced long before the end of their service life. Airline companies and air forces sometimes base their repair and maintenance intervals on the intervals supplied by the experiences of other users. The operational use of the gas turbines usually differs between most users. It would therefore be much more attractive to base the repair and maintenance inspection intervals on actual usage by monitoring all separate engines (usage monitoring), which is called on-condition maintenance.

1.2 The research project

The main purpose of this project is to find out whether a propagation lifetime can be calculated for a complex gas turbine component. As a case study, the propagation lifetime of a 2^{nd}-stage fan disc of the Pratt & Whitney F100-PW-220 gas turbine is determined. This component is described section 2.3. Although the nomenclature indicates a lifetime calculation of the disc, the actual lifetime of the hub will be determined. Because this hub is a part of the fan disc, the component is called 2^{nd}-stage fan disc. To determine the propagation lifetime a certain course, or solution strategy must be followed. This project is mainly used to determine the course and see whether it can produce acceptable solutions, provided that there is enough data known. To determine the propagation lifetime, data like the initial crack size, the crack growth behaviour, and several other aspects must be investigated. The main aspects of the research are investigation of:

- **The load spectrum**

  The load spectrum that is applied during service must be examined to see which load or combination of loads is the cause of the failure of the compressor fan disc. The load spectrum used in this calculation will be based on usage data of the Royal Netherlands Air Force (RNLAF), and will form the base of the crack growth calculation. It is therefore of great importance to generate a representative load sequence, based on the use of the RNLAF, as input for the crack growth calculation.

- **The materials crack growth behaviour**

  The fan disc material must be analysed to determine a relation between the crack growth rate (da/dN) and the load parameter (ΔK).

– **The stress intensity factor solution**
  A stress intensity factor solution (SIF- or K-solution) relates the stress at the crack tip to the remote load, based on geometry, load, crack length, and location of the crack. The SIF-solution will be determined using a simplified finite element (FE) model of the hub of the fan disc.
– **Stop criterion for the crack growth calculation**
  Failure or rejection of the component can be the result of different mechanisms. Which mechanism or cause causes the component to fail or be rejected must be investigated.

When these aspects are investigated they can be used to determine a deterministic crack growth lifetime.

1.3 Stochastic Fatigue Analysis

Fatigue analyses are usually performed as deterministic analyses, implying that variability of different parameters is not taken into account. The elastic modulus of a material for instance, is usually taken as a constant, but in practice it varies between a minimum and a maximum value. Parameters as material properties, sizes, loading, etc. are often uncertain and not constant. Dealing with the variability of the parameters a new kind of analysis, namely the stochastic analysis, is introduced. This type of analysis gives the deterministic analysis an extra dimension by generating solutions with a probability interval. Dealing with the uncertainties, a much more probable answer is obtained. [Ref. 1]

The next list of factors is solemnly shown to indicate that there are many uncertainties that could influence the lifetime calculation. [Ref. 2]

Metallurgical and processing variables

- alloy composition,
- microstructure,
- batch (heat-to-heat variation),
- distribution of alloy elements,
- grain size,
- preferred orientation (texture),
- product form,
- orientation with respect to grain direction,
- heat treatment,
- mechanical or thermal-mechanical treatment,
- residual stress,
- manufacturer.

Geometrical variables

- thickness,
- crack geometry,
- component geometry,
- stress concentrations (e.g., the presence of a notch, holes, etc.).

Mechanical variables

- cyclic stress amplitude (R-ratio),
- loading condition (biaxial load, load transfer, etc.),
- cyclic load frequency, wave form, and hold time,
- load interactions in spectrum loading,
- pre-existing residual stress.

Environmental variables

- type of aggressive environment (gas, liquid, liquid metal, etc.),
- concentration of aggressive species,
- electrochemical potential,
- temperature,

1.4 Structure of the report

The report is divided into 7 main chapters. In the first chapter a brief introduction is given on the objective and the reason of the project. In the second chapter a brief introduction of the F-16 and the Pratt & Whitney F-100-PW-220 is given. This section also describes the geometry of the 2^{nd}-stage fan disc, and the failure of an American gas turbine. Before the actual research is discussed, some elementary theory of life prediction methods and fracture mechanics will be discussed. Chapter 3 describes the various life prediction philosophies, and the philosophies used by Pratt & Whitney for the F-100-PW-220 gas turbine. The lifetime calculation is based on crack growth. Therefore the theory of fracture mechanics is discussed in chapter 4. The actual conducted research is described in chapter 5, which discusses the various aspects which must be investigated prior to the crack growth calculation. The results and the discussion of the results are given in chapter 6. Finally conclusions and recommendations are given in chapter 7.

2 The F-16, a multi-role fighter aircraft

2.1 The Royal Netherlands Air Force

In 1974 the department of defence decided to replace the Starfighter of the Royal Netherlands Air Force (RNLAF) with a modern fighter jet. On the 27th of May 1975 the General Dynamics F-16 Falcon (see figure 1) was chosen to become the fighter for the future. A first order of 84 aircraft was placed, with an option to expand the fleet with more aircraft. The first two F-16's were assigned to Leeuwarden airfield. These two aircraft, a single and a dual seater, assembled by Fokker, were delivered on the 6th of June 1979. The total fleet of the RNLAF consists of 213 F-16's. (These will not be in service at the same time, and includes replacements for the calculated 30 aircraft which could be lost in peace-time due to failure.) The Starfighter was taken out of service in 1984, and the NF-5 followed in 1991.

Fig. 1 The General Dynamics F-16 fighter aircraft

During their service the F-16's have been modernised twice. First, a dragchute was added to the tailplane, and nowadays the F-16's receive the Mid Life Update. During the Mid Life Update (MLU) all electronic systems are replaced, the cockpit is rearranged to increase the user-friendliness, and a Fatigue Analyzer and Autonomous Combat Evaluation system, FACE, is added. A total of 128 Mid Life Updated F-16's remain in service until their successor (possibly the Joint Strike fighter, JSF) arrives towards the year 2008/2010.

Till then the F-16's must be operated both economicly and safely. This implies that the current life must be expanded until the replacements arrive. To meet the safety requirements, the repair and maintenance schedule has to be altered, and all components, that are likely to fail, have to be revised. This is applicable to both airframe and engine. Currently the F-16's are powered by Pratt & Whitney F100-PW-220 turbofan engines.

2.2 Pratt & Whitney F100-PW-220 turbofan gas turbine

The F-16's of the Royal Netherlands Air Force are equipped with Pratt & Whitney F100-PW-220 turbofan engines, of which a cut away picture is shown in figure 2. To improve the performance of the gas turbine, i.e. the thermal efficiency, a high pressure ratio is essential. Axial compressors are used to compress air efficiently, and many compressor stages are needed to obtain a high pressure ratio. The problem with axial compressors is that if they are operated at low rotational speeds (well below the design value) the air density in the last few stages is much to low, and blades will stall due to excessive axial flow velocity. The unstable region (manifested by aerodynamic vibration) is encountered when a gas turbine is started up or operated at low power. To overcome this problem compressors are mechanically partitioned into two or more sections. These compressor sections usually operate at different rotational speeds, so each compressor section will be powered by its own turbine. The low-pressure compressor is driven by the low-pressure turbine, and the high-pressure compressor is driven by the high-pressure turbine. This configuration is usually referred to as a *twin-spool* gas turbine. [Ref. 3]

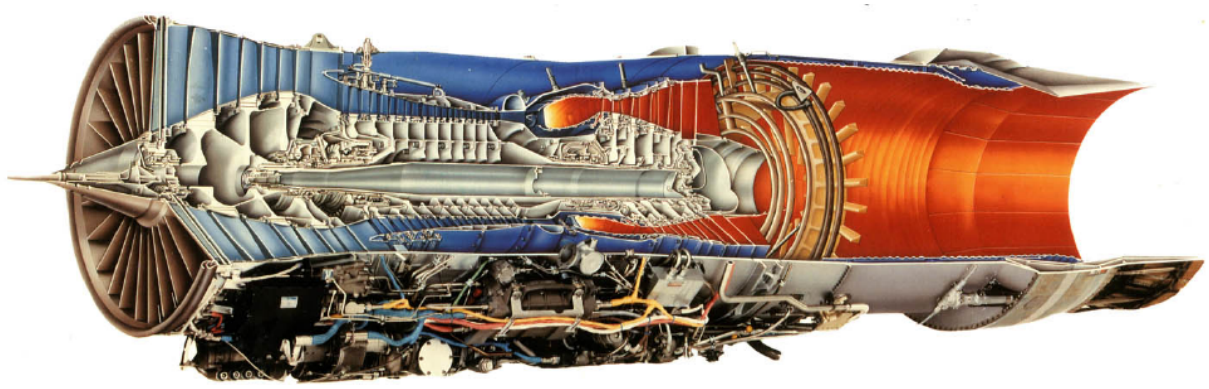

Fig. 2 Cut away view of the Pratt & Whitney F100-PW-220

The low-pressure compressor is referred to as the fan. The Inlet Fan Module (IFM) is located at the front of the F100-PW-220 engine, and delivers compressed air to the high pressure compressor. There are three rows of rotor blades, two rows of vanes, and one row of inlet guide vanes in the in the fan module. The first, second and third stage blades are mounted respectively on the first, second and third stage fan disc. The 1^{st}-stage and 3^{rd}-stage fan disc are bolted to the 2^{nd}-stage fan disc. The 2^{nd}-stage fan disc is connected to the low pressure shaft through the hub. Figure 3 shows a half cross section of the fan module. In the past, the United States Air Force (USAF) experienced an accident which was due to crack propagation from one of the thrust balance holes in the hub of the 2^{nd}-stage fan disc.

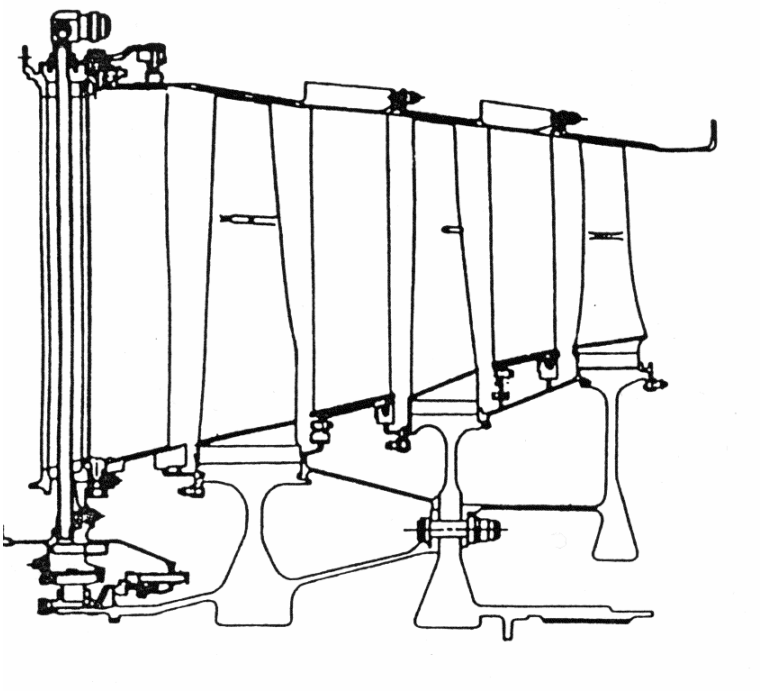

Fig. 3 Fan module of the F100-PW-220

2.3 Failure of the second stage fan disc

To perform a risk assessment analysis, a deterministic analysis must be made first. In addition to the deterministic analysis a stochastic fatigue analysis can be performed, which wil not be part of this investigation. Due to some problems with the 2^{nd}-stage fan disc of the Pratt & Whitney gas turbine, RNLAF planned risk assessment analysis for this specific component.

There has been one reported fracture of a 2^{nd}-stage fan disc and hub due to a fatigue crack which grew from one of the 21 thrust balance holes in the direction of the spline (towards the back of the gas turbine). The event occurred in a development engine on a ground test stand engine that was subjected to an accelerated mission test.

The current 2^{nd}-stage fan disc in the F100-PW-220 of the RNLAF is a redesign of the original fan disc design. In this report the second design (redesign) is used for the deterministic fatigue analysis for two reasons. The first reason is that the second design is the actual disc in the gas turbines of the RNLAF. The second, main reason, is that it can be used to prove that calculations like these are possible to perform. A complementary advantage is that the second design is reasonable simple due to its relatively simple configuration compared to other designs. If the analysis can be made, more complicated models can be analysed using the same solution strategy.

The second design of the 2^{nd}-stage fan disc, as well as the 1^{st}-stage and 3^{rd}-stage discs and their interconnection are shown in figure 4, which shows the rotor part of the IFM.

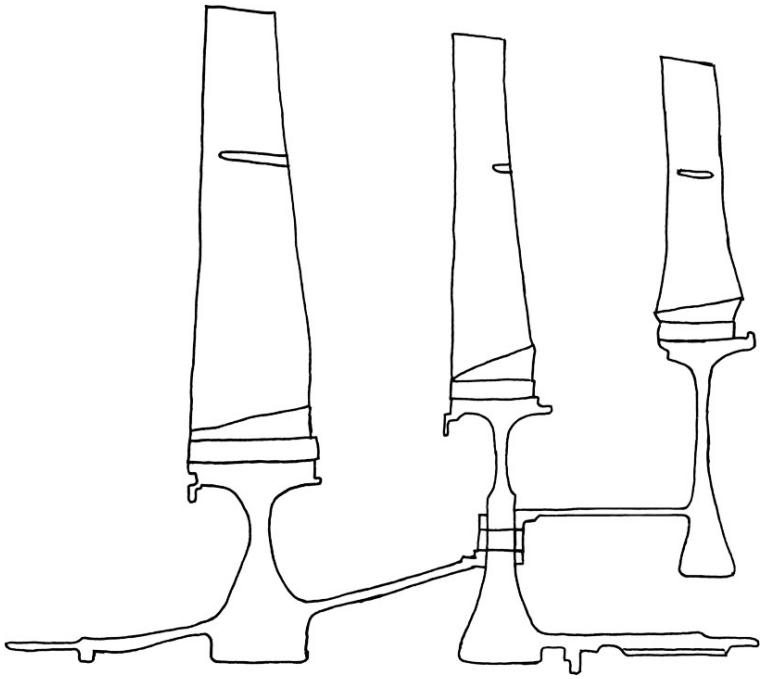

Fig. 4 Interconnection of 1^{st}-, 2^{nd}-, and 3^{rd}-stage fan disc

In this report technical expressions like hub, thrust balance holes, spacer/holder, etc. are used. The used expressions in this report are shown in table 1. The numbers correspond with the numbers in figure 5. [Ref. 4]

Table 1 Nomenclature of 2^{nd}-stage fan disc

number	designation
1	thrust balance holes (#21)
2	hub
3	spline
4	spacer/holder
5	bore
6	web bolthole
7	web
8	live rim
9	scallop

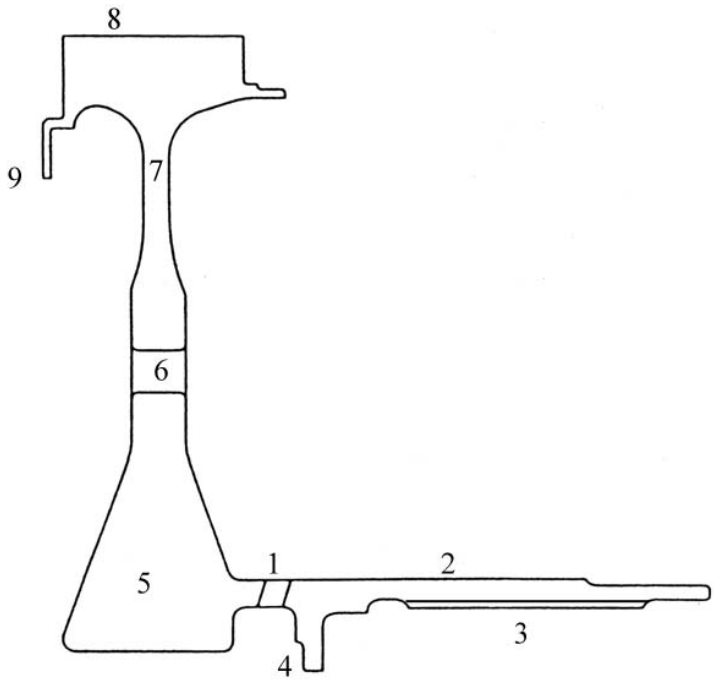

Fig. 5 Nomenclature of 2^{nd}-stage fan disc

3 Life prediction

3.1 Introduction

Before discussing fracture mechanics, which is the basis for the fatigue lifetime calculation, fatigue design philosophies will be discussed. Over the years (since the 1950s) several design philosophies have been developed. The first design philosophy was the traditional *safe-life* approach. This design philosophy treats aircraft structures to be designed for a finite service life, during which significant fatigue damage will not occur. Basic to this approach is that either the structure is not inspectable or that no inspections are planned during the service life.

3.2 Fatigue design philosophies

Various design philosophies have been developed for dealing with the problem of loss of structural strength due to the initiation and subsequent growth of cracks by fatigue. In the early 1960s a design philosophy known as *fail-safe* was developed. With this philosophy a structure is designed to have an adequate life free from significant fatigue damage, but continued operation is permitted beyond the life at which such damage may develop. Safety is incorporated into the *fail-safe* approach under the assumption that any fatigue crack that is developed will be detected by routine inspection procedures before they result in a dangerous reduction of the static strength of the structure. Two requirements

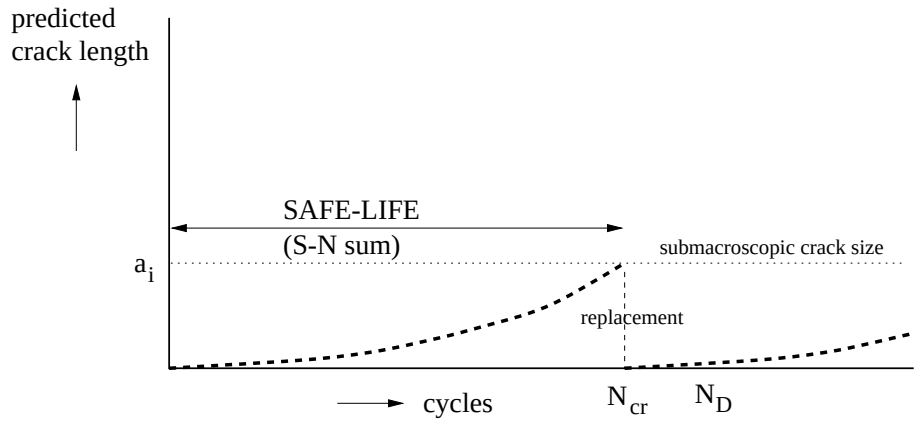

Fig. 6 Safe-Life design philosophy

are necessary for this approach to be successful. First, a minimum crack size must be defined which will not go undetected at a routine inspection. Second, a prediction of the crack growth rate until the next inspection must be defined.

In the early 1970s another design philosophy was proposed. The object of which was to design a damage tolerant structure. This philosophy is similar to the *fail-safe* approach, but differs from the original *safe-life* approach on two major aspects. First it is assumed that flaws or cracks are present in the structure as manufactured. These flaws or cracks may arise from metallurgical imperfections in the material, or from manufacturing faults. The second aspect is that structures may be inspectable or non-inspectable. This design philosophy is called the *damage-tolerance* design philosophy.

The application of the *damage-tolerance* approach to a given component depends on whether the component is classed as *inspectable* or *non-inspectable* during routine service inspections. For components that are inspectable the procedures closely follow those used in *fail-safe* design. However, in the case of non-inspectable parts it must be demonstrated that the time for the crack to grow to failure, from the prescribed initial flaw, is greater than the desired service life.

For military gas turbine engines, the majority of components is treated according to the *safe-life* design philosophy, so that the components are treated to be free of initial defects or discontinuities and no planned inspections are going to be done. The USAF and Pratt & Whitney Aircraft use for some of their components the *damage-tolerance* design philosophy.

3.3 Pratt & Whitney Aircraft life prediction interpretation

The life prediction according to Pratt & Whitney Aircraft starts with the designation of components to be either *fracture critical* or *durability critical*. The fracture critical designation is used for components if its failure results in a total loss of the engine and the inability to continue safe operation of the

aircraft. The durability critical designation for components is used when failure of the components lead to significant maintenance without jeopardising flight safety. All gas turbine components are subjected to a durability limit calculation. The durability limit (or the economic life limit) presents, according to Pratt & Whitney, the point in time where it would be more economic to replace a component than to continue inspection or repairs. For fracture critical components, also a safety limit is calculated. This safety limit is considered to be the time beyond which the risk of components failure is considered to be unacceptably high if corrective actions are not taken. This time is based on the time required for the maximum probable initial flaw or defect to grow to critical condition and cause component failure. The safety limit must always be lower than the durability limit and will be used to determine the inspection intervals. Usually the inspection interval is half the safety limit. In general the Low Cycle Fatigue (LCF) life limit is used as the durability limit. Several approaches to determine this life limit exist.

3.3.1 Safe-Life design philosophy

The conventional safe-life design philosophy equals the life limit to the LCF life limit, which is calculated with the aid of S-N curves (these curves describe the relation between the fatigue life and the stress level for a given stress concentration factor). The LCF life limit is associated with the time to initiate a $\frac{1}{32}$ inch long surface crack in a part with no pre-existing defect. The LCF life limit is determined with the use of a large amount of test data, which gives a distribution of crack initiation lives. (See figure 6) For the LCF life limit the B.1 value (this is the lifetime wherein 1 out of 1000, or 0.1%, of the test samples a crack has initiated) is used. (See figure 7)

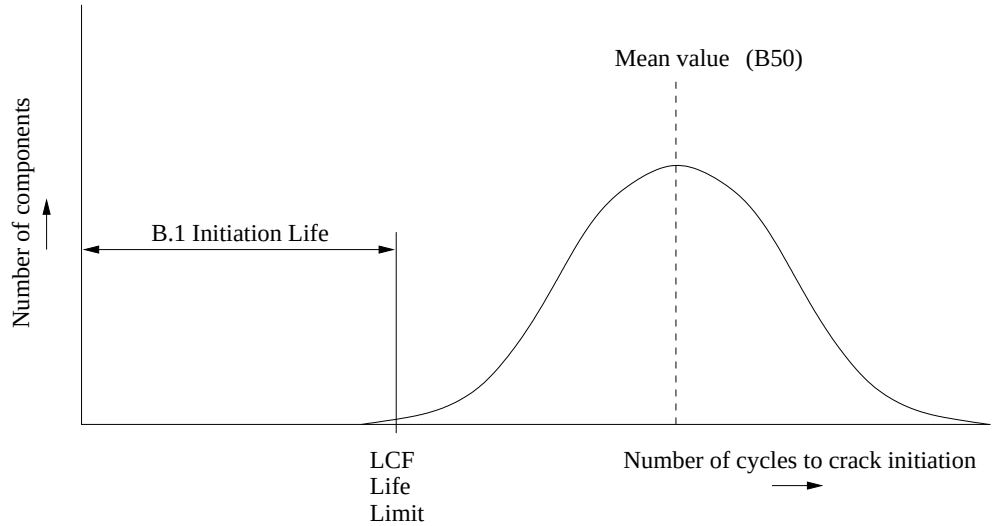

Fig. 7 PWA Safe-Life approach

3.3.2 Damage Tolerance design philosophy

The initial lifetime calculation (called the initiation life) of the damage tolerance approach is similar to the calculation following the safe-life approach, but in addition a potential life extension will be calculated (called the propagation life). This lifetime extension is done by calculating the time for a crack of minimum detectable NDI size to grow to the critical crack size. The total lifetime will be calculated as follows:

$$(LCF)\ life\ limit = B.1\ Initiation\ Life\ + B.1\ Propagation\ Life \tag{1}$$

The B.1 value of the initiation life is similar to the value used in the safe-life approach. The propagation life is obtained in a similar way where 1 out of 1000 components has reached the critical crack length, for which a large amount of test data is necessary. This limit, the B.1 propagation life limit is also called the safety limit. To actually determine the propagation life several requirements are needed, such as; service loads, crack propagation rate, critical crack size, initial crack size, and the stress intensity factor solution.

During service life, inspection intervals are planned. If cracks are found during inspection the concerned component will be rejected and replaced. The first inspection interval is recommended to be 0.5 to 1.0 times the calculated safety limit. If no cracks or flaws are found with the current NDI methods, the minimal detectable crack or flaw size of the inspection method is assumed to exist. From this point the inspection interval is also recommended to be 0.5 to 1.0 times the calculated safety limit. The chance that a component with a crack is found is relatively small because of the B.1 values of the initiation and propagation life. The initiation life and the propagation life are assumed to be independent according to Pratt & Whitney Aircraft, so the total risk of finding a cracked component will be one in a million. If no defects or cracks are found during inspection intervals, but the lifetime is reached, the component will also be retired. The major disadvantage of the damage tolerance approach is that most of the components are retired in a premature stage, meaning that the components are retired in an uncracked state. Due to the high rate of conservatism an additional, third approach, was developed. (See figure 8)

3.3.3 Retirement For Cause design philosophy

Due to the damage tolerance approach (equation 1) most components are replaced prematurely. This means that a small part of the potential life capacity of the components is used. The fundamentals of the retirement for cause approach are based on life extension beyond the LCF life limit of the damage tolerance approach. This design philosophy does not imply that each individual component can be

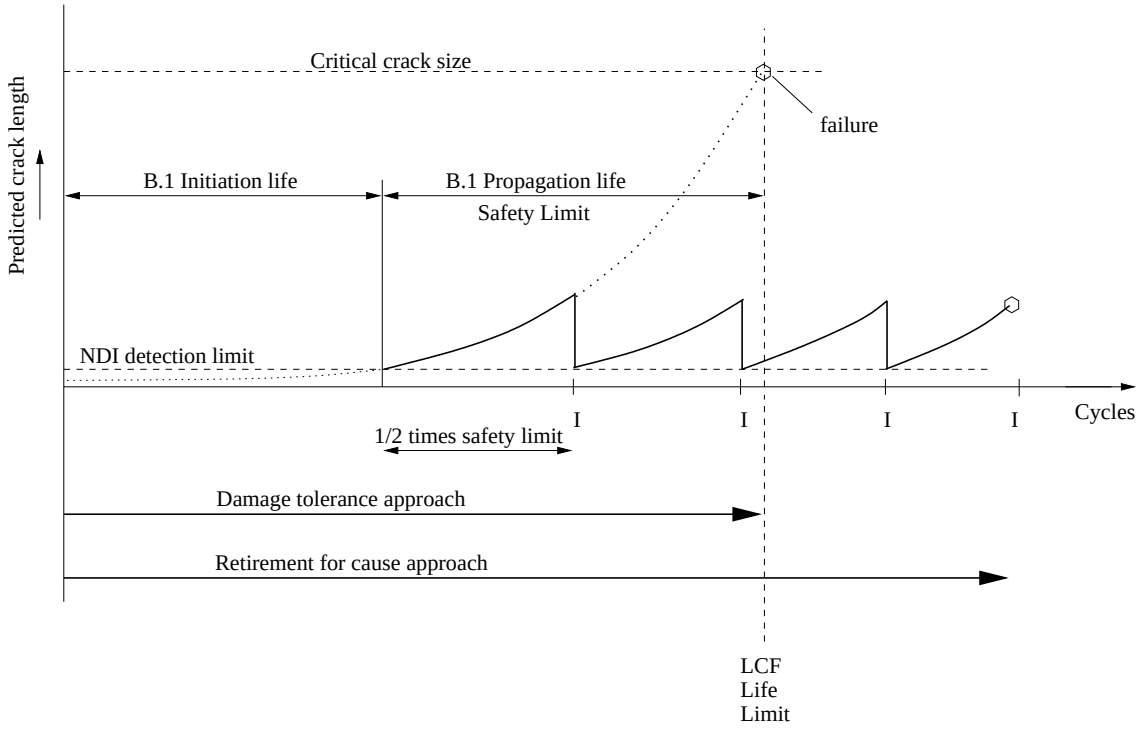

Fig. 8 PWA Damage Tolerance and Retirement For Cause approach

used until a crack is detected and that the full life capacity can be used. There are two reasons for not utilizing the full life capacity. The first reason is that it is possible not to detect internal defects during inspection. The second reason is that the risk of missing a crack increases with increasing life. In contrast to the damage tolerance approach, the (risk analysis of the) Pratt & Whitney Aircraft retirement for cause approach gives the exact risk. At first the maximum acceptable risk is determined and then a statistical risk analysis is used to calculate how many components may contain a crack before the whole set of components is retired. Pratt & Whitney Aircraft therefore uses this retirement for cause approach to increase the LCF life limit, but when a component has reached this limit, it is retired, whether or not it contains a crack. (See figure 8) [Ref. 5, 6]

3.4 Life prediction for the 2^{nd}-stage fan disc

In case of the 2^{nd}-stage fan disc the damage tolerant design philosophy is used to perform the life prediction. The propagation life limit must be determined, which will be based on crack growth from the initial crack length to the critical crack length.

4 Fracture mechanics

4.1 Introduction

In order to determine the expected life of components that are likely to fail due to crack extension, data of materials' resistance to crack growth, geometry features and loading cycles must be known. These data must then be analysed and verified according to certain theories to determine the rate of crack growth. In order to use these theories some basic understandings of fracture mechanics is needed.

4.2 Failure modes

Many failures of engineering components and structures are due to fracture by the propagation of cracks. The way in which a crack propagates depends on the applied loading. Three distinct modes of fracture are likely to occur. These three distinct modes of fracture are shown in figure 9. When a

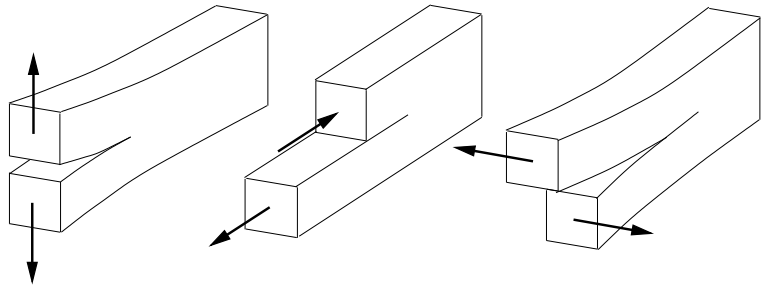

Mode I Mode II Mode III

Fig. 9 Three distinct modes of fracture

crack is subjected to, and normal to, a tension load which pulls the crack surfaces directly apart, the corresponding fracture mode is called the tensile mode, opening mode, or mode I. The accompanying index i for the stress intensity factor is *I*. The significance of the stress intensity factor, which is often abbreviated as SIF or as K_i, is explained in the next section. The fracture mode that is characterised by displacements in which the crack surfaces slide over each other in the direction perpendicular to the crack front is called the shear mode, sliding mode, or mode II. The accompanying index i for the stress intensity factor is *II*. The last fracture mode is called the tearing mode, torsion mode, or mode III. The crack surfaces in this mode slide opposite to each other in the direction parallel to the leading edge of the crack. The accompanying index i for the stress intensity factor is *III*.

Although crack propagation in mode I is the most common type of fracture, and therefore the most important, specific load cases can lead to stress distributions at the crack tips which are combinations of all three modes.

The distinct modes of fracture can be divided in either stable or unstable crack propagation. Unstable

crack growth, also known as fast fracture, frequently has catastrophic consequences and is sometimes referred to as brittle fracture. (Because there is usually very little plastic deformation of the material in the vicinity of the crack) All components contain, besides stress concentrations (due to geometric features), imperfections in the material which must be regarded as potential cracks. It is very important to be able to predict when fast fracture is likely to occur. Stable crack growth is also of considerable importance. Under fatigue conditions of repeated cyclic loading, such growth is often unavoidable and may lead to eventual fast fracture. The ability to predict rates of crack growth is therefore highly desirable, in order to determine the service life of a component. [Ref. 2, 7]

4.3 The stress intensity factor

The application of fracture mechanics relies on the stress intensity factor. An important part of the solution of fracture problems in linear elastic fracture mechanics (LEFM) is determining the stress intensity factor (SIF or K). The stress intensity factor is actually a physical quantity, not a factor. A factor (e.g., the stress concentration factor, K_t) is by definition unitless (or dimensionless). It is clearly shown in equation A.3 of appendix A that K has a unit of stress times the square root of the crack length. This quantity is needed to balance the stress on the left, and the $1/\sqrt{r}$ on the right. In appendix A the stresses and the displacements near the crack tip are described. K has been called the stress intensity factor because it appears as a factor in equation A.3 of appendix A. Usually K is often expressed as a solution where many dimensionless factors are taken into account for the used geometry. The SIF not only characterises the stress and displacement distributions at the crack tip, it also characterises the behaviour and the criticality of the crack. The solution for K consists of terms representative of stress (or load), crack length, and geometry. It accounts for the geometry of a local area in a structure and how the load is applied. The general expression for K can be written as:

$$K = S\sqrt{\pi a} \cdot \phi_1 \cdot \phi_2 \cdot \phi_3 \cdot \phi_4 \ldots \tag{2}$$

In this equation S is the (remote) load, a the crack length, and the ϕ_i's are normally expressed as dimensionless geometric parameters (e.g. crack length to specimen width ratio, specimen width to length ratio, etc.). Due to the relatively complicated nature of the considered component, a stress intensity factor is normally obtained for a stationary configuration (i.e., a fixed crack length in a geometry having fixed dimensions) with the use of Finite Element Methods (FEM). Each SIF is obtained by solving one cracked problem at a time using a FEM program. The SIF-solution, which is a curve where the SIF is plotted against the crack length, is obtained by fitting a curve through several calculated stress intensity factors for several crack sizes. [Ref. 2]

4.4 Fatigue crack propagation

Many structural failures are the result of the growth of pre-existing subcritical flaws or cracks to a critical size under fatigue loading. The growth of these flaws will occur at load levels well below the ultimate load that can be sustained by the structure. A quantitative understanding of this behaviour is required before the performance of the structure can be evaluated. Information on the crack propagation behaviour of metals is needed for selecting the best-performing material, evaluating the safe-life capability of a design, and establishing inspection periods. [Ref. 2, 7]

4.5 Fatigue loading

Fatigue crack propagation is a phenomenon in which the crack extends at every applied stress cycle. A clear illustration of this phenomenon is shown in a fractograph (see figure 10) that was taken from the fracture surface of a specimen after the specimen was terminated from a cyclic crack growth test. The loading block contained 24 constant-amplitude stress cycles in which 3 of the cycles had a lower mean loading than the others. The magnitude of the amplitudes of all the individual cycles is thus equal, except for the transition to higher mean loading, where the total amplitude is larger. This results in a larger striation mark on the fracture surface. The amount of crack extension due to a stress cycle can be calculated by measuring the width between two large striation marks, and dividing this distance through the number of cycles. In this case the total number of load cycles between the two large striation marks is 23.

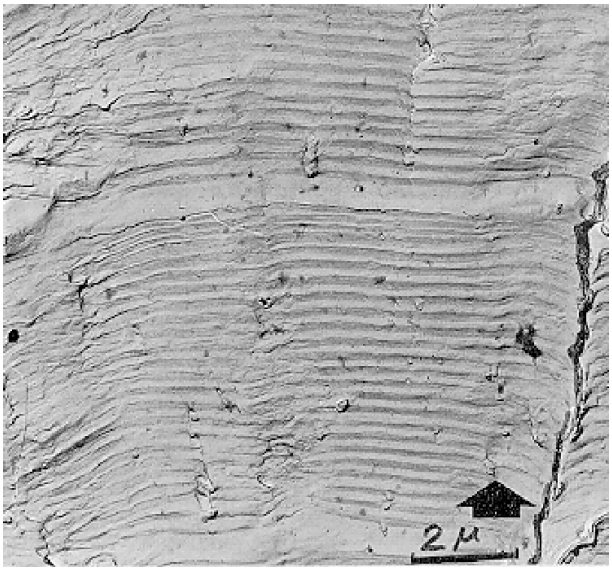

Fig. 10 Fractograph showing striation markings of fatigue loading cycles

The loadings on structures and components are often of variable nature. This implies that loadings during the lifetime differ due to in-service applications. The applied load case during the lifetime consists of high, low, and compression loads, and is one of the key elements that controls crack

growth behaviour. Higher load levels speed up the crack growth process while compressive load levels will delay crack growth propagation. Due to high loads, the vicinity of the crack tip will show plastic deformation, causing lengthening of the material, and thus internal stresses. When the loads are reduced the crack will close under the influence of the internal stresses and stay dormant for a period of time. After a certain number of cycles the crack will resume its normal growth behaviour again. The delay depends on the level of the stress and the difference between the stress levels for a given material. This phenomenon is called $delay$, but is better known as *crack growth retardation*. [Ref. 2]

4.6 Crack growth formulation

This section discusses the techniques to describe or to present crack growth data. In the first subsection a brief overview of the general approach of describing crack growth data is shown. The second subsection discusses the complicated, collective techniques to present the crack growth data.

4.6.1 Individual crack growth formulation

The methods for conducting fatigue crack growth testing as well as data reduction procedures are specified in ASTM E 647. Fatigue crack growth testing can be conducted on any type of test specimen or structural component. Either compact specimens or centre-cracked specimens can be used for generating material da/dN data. Tests are run under constant-amplitude loading, i.e., the maximum and minimum load levels are kept constant for the duration of the test. Either a sinusoidal or saw-tooth wave form is used for fluctuating the input loads. The data recorded from the test include the testing parameters as well as the crack length as a function of the number of cycles. The crack growth data are usually obtained by visually measuring the crack length and noting the number of load cycles on a counter. Crack gages or compliance techniques can be used instead of visual measurement to monitor the progress of crack propagation. This gives a series of points that describe the crack length as a function of load cycles for a given test.

Crack growth rates are computed on every two consecutive data points. The amount of each crack growth increment is Δa. The difference in the number of fatigue cycles between two consecutive data points is ΔN. Dividing Δa by ΔN will produce the crack growth rate per cycle.

Stress intensity factors, corresponding to each increment of crack growth are computed using the average crack length of each pair of consecutive data points. Alternatively, one may prefer to draw a smooth curve through the a versus N data points first, then determine the slope for each selected point on the curve. The slope of a given point on the smooth curve is the da/dN for that point. The K_{max} and K_{min} values corresponding to each of these crack lengths also can be determined.

The rate of crack growth, da/dN, is a function of K_{max} and K_{min}. Letting:

$$\Delta K = K_{max} - K_{min} \tag{3}$$

and

$$R = K_{min}/K_{max}. \tag{4}$$

The relation between da/dN and K can be expressed as:

$$\frac{da}{dN} = f(\Delta K, R) \tag{5}$$

or

$$\frac{da}{dN} = f(K_{max}, R) \tag{6}$$

For zero-to-tension loading, i.e., $R = 0$, these two equations are identical. Therefore, da/dN can be plotted as a function of ΔK, or K_{max}. It has become a standard practice to use ΔK as the independent variable for data presentation. A set of typical da/dN versus ΔK data (plotted on a log-log scale) for a 7075-T6 alloy, is shown in figure 11. To put da/dN and ΔK in an equation, Paris described the fatigue crack growth rate data by a power law equation:

$$\frac{da}{dN} = C(\Delta K)^n \tag{7}$$

where n is the slope and C is the coefficient at the intercept of a log-log plot. The Paris equation shows that there is a linear relationship between da/dN and ΔK, which can be visualised on a log-log plot. Diversification in crack growth rate description is necessary because each individual investigator faces a situation that is unique to the material and application associated with the product of a particular industry.

The mean stress is defined as the average of the maximum and minimum stress of a given fatigue

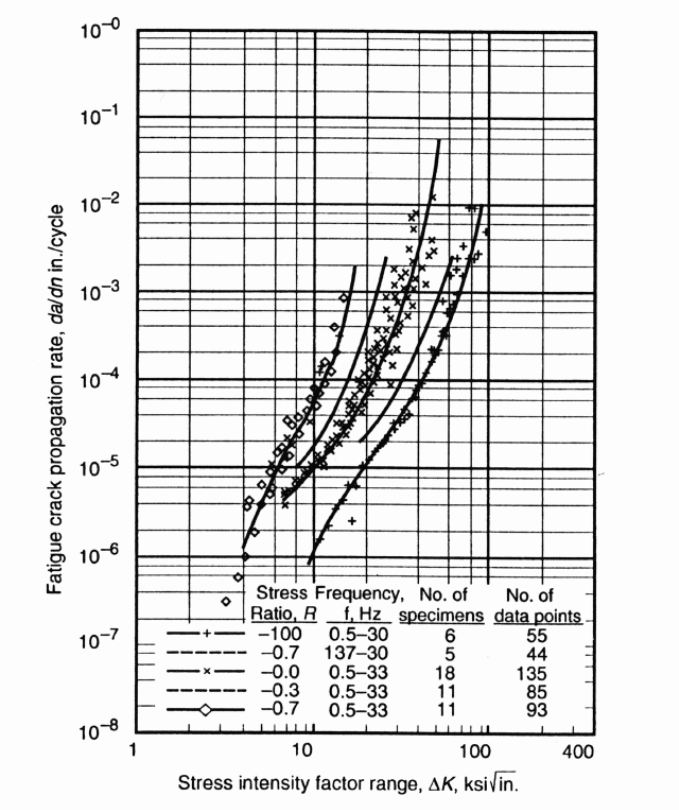

Fig. 11 Fatigue crack growth rate data

cycle. When two tests at different mean stress levels are conducted (e.g., they have the same ΔS but different R ratios) the cyclic crack growth rates will not be the same. Referring to the fractograph of figure 10, the striation band corresponding to the cycle of lower mean stress is narrower than the striation band for the cycle that has a higher mean stress level. This means that the fatigue crack growth rate for the former is lower than for the latter. This phenomenon is called the mean stress effect, or stress ratio (R-ratio) effect. Using Paris' equation (equation 7), one can only plot a da/dN curve for a given R-ratio. Eventually a series of equations is needed to fully describe the da/dN behaviour for a wide range of stress ratios. This means that different pairs of C and n values are needed for each equation (for a particular stress ratio). This type of data presentation is called correlating the data *individually*, because each set of data points corresponds to a certain value of R. (See figure 11) In addition to the mean stress effect, there is another element that is inherently associated with the da/dN data and needs to described. In general, a da/dN curve appears to have three regions. The first region is a slow-growing region (the so-called threshold), the second region is a linear region (the middle section of the curve, described by Paris), and the third region is a fast-growing region (towards the end of the curve where ΔK approaches the critical fracture toughness, K_c). A smooth connection of all three regions forms a sigmoidal curve representative of the entire da/dN versus ΔK curve for

a given R. Figure 12 shows a simplified crack growth curve. Although some alloys may not exhibit a clearly defined threshold, i.e., the entire da/dN curve is apparently linear up to the termination point, the existence of these regions has been well recognized.

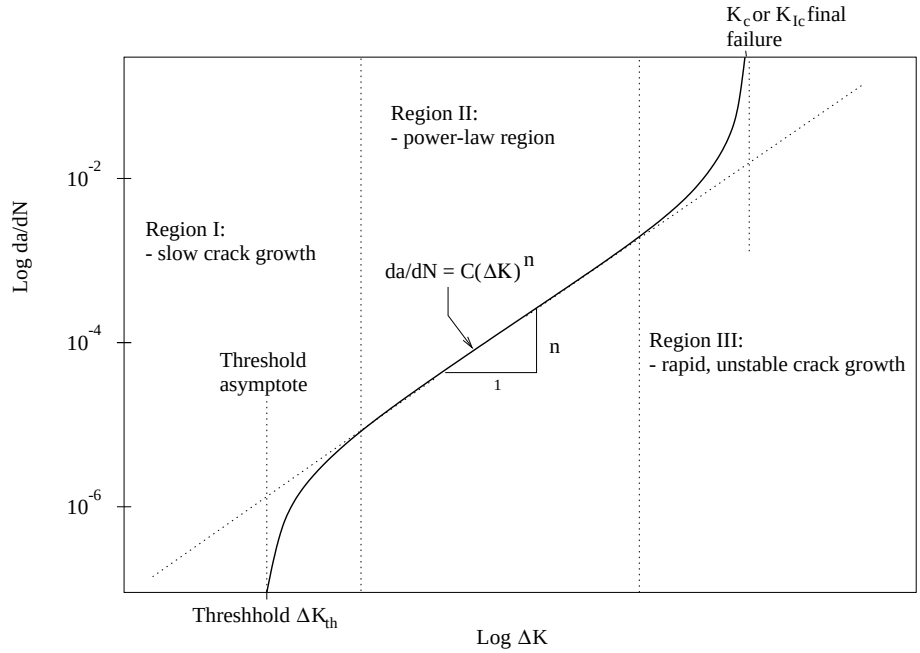

Fig. 12 Multiple region fatigue crack growth rate curve

The physical significance of the slow-growing and terminal (critical) region is that there are two obvious limits of ΔK in a da/dN curve. The lower limit (the threshold value ΔK_{th}) implies that cracks will not grow if ΔK is smaller than ΔK_{th} i.e., $da/dN \rightarrow 0$ when (ΔK - ΔK_{th}) $\rightarrow 0$. If ΔK becomes too high, implying that K_{max} exceeds the fracture toughness K_c, static failure will follow immediately. This is equivalent to ΔK exceeding $(1-R)K_c$ i.e., $da/dN \rightarrow \infty$ when $[(1-R)K_c - \Delta K] \rightarrow 0$. With these additions added to the Paris' equation (equation 7), a sigmoidal relation on a log-log plot with two vertical asymptotes will be obtained as:

$$\frac{da}{dN} = C(\Delta K)^n \frac{\Delta K - \Delta K_{th}}{(1-R)\,K_c - \Delta K} \tag{8}$$

The values C and n are respectively the intercept and slope of the line that fits through the linear region of the da/dN curve. The $(1-R)$ term in equation 8 is pure for providing the termination point of the da/dN curve. It does not form any connection between da/dN at different R-ratios. Therefore equation 8 can only be used for correlating the data individually (i.e., with one R-ratio at a time).

Two problems in describing crack growth rate data are faced. The first is establishing a relationship

between all the stress ratio's in obtaining a mathematical function that translates all the da/dN data points into a common scale. The advantage of this translation is that only one pair of C and n values is needed for the entire data set. This approach is called correlating the data *collectively*. The second problem is the need to select a curve-fitting equation capable of fitting through all three regions of the da/dN data. Among the many crack growth rate equations published in the literature, some deal with the mathematical formulation of a sigmoidal curve, or normalizing the stress ratio effect, or both. Some even divide the da/dN curve into multiple segments, attempting to obtain a closer fit between experimental data and a set of equations. [Ref. 2] The next section will discuss in what way these problems are dealt with by using different crack growth relations, based on collective data presentation.

4.6.2 Crack growth relations for collective data presentation

At NLR the program CRAGRO, which is a modification of NASA's NASGRO 3.00, is used for crack growth calculations. This program is based on fracture mechanics principles and is used to calculate stress intensity factors, to compute critical crack sizes, or to conduct safe-life analyses. For this program an advanced crack growth relation was developed to present data collectively.

Crack growth relation

The crack growth rate calculations the program uses were developed by Forman, Newman at NASA, De Koning at NLR and Hendriksen at ESA. This equation (equation 9) describes the behaviour of the three regions of crack growth similar as equation 8, but differs slightly because this equation presents the data collectively. [Ref. 8]

$$\frac{da}{dN} = C(\Delta K)^n \frac{(1-f)^n}{(1-R)^n} \frac{\left(1 - \frac{\Delta K_{th}}{\Delta K}\right)^p}{\left(1 - \frac{\Delta K}{(1-R)K_c}\right)^q} \tag{9}$$

The equation uses constants C, n, p, and q which must be empirically derived. The f in the equation is the crack opening function for plasticity-induced crack closure defined by Newman. [Ref. 9]

$$f = \frac{K_{open}}{K_{max}} = \begin{cases} maximum\left(R, A_0 + A_1 R + A_2 R^2 + A_3 R^3\right) & \text{if} \quad R \geq 0; \\ A_0 + A_1 R & \text{if} \quad -2 \leq R < 0. \end{cases} \tag{10}$$

The coefficients used by equation 10 are given by;

$$\begin{aligned} A_0 &= (0.825 - 0.34\alpha + 0.05\alpha^2)\left(\cos\left(\tfrac{\pi}{2}\tfrac{S_{max}}{\sigma_0}\right)\right)^{\frac{1}{\alpha}} \\ A_1 &= (0.415 - 0.071\alpha)\,\tfrac{S_{max}}{\sigma_0} \\ A_2 &= 1 - A_0 - A_1 - A_3 \\ A_2 &= 2A_0 - A_1 - 1 \end{aligned} \tag{11}$$

In these equations, α is the plain stress/strain constraint factor, and S_{max}/σ_0 is the maximum applied stress to the flow stress. Both α and S_{max}/σ_0 are dependent on the used material.

It was shown that the lower asymptote was formulated by the threshold stress intensity factor (ΔK_{th}). The threshold stress intensity factor is approximated as a function of the stress ratio (R), the threshold stress intensity factor at $R = 0$ (ΔK_0), the crack length a, and the intrinsic crack length (a_0):

$$\Delta K_{th} = \Delta K_0 \left(\frac{4}{\pi}\tan(1 - R)\right)\sqrt{\frac{a}{a + a_0}} \tag{12}$$

The applied ΔK appears to differ from the actual ΔK which acts on a stress cycle. This difference may vary for different R-ratios. In order to account for the mean stress effect on da/dN, a method to estimate the effective level of applied K for a given R-ratio must be developed. The method that accounts for this effect is known as the concept of crack closure. It has been developed for a relation between the effective ΔK and R.

Effective ΔK

The concept of crack closure assumes that material near the crack tip is plastically deformed during the fatigue crack propagation. Releasing the pressure (during unloading of a fatigue cycle), some contact will occur between the faces of the crack surfaces due to elastically deformed material in the surroundings of the crack tip. If the component is loaded in the following fatigue cycle, the faces of the crack will not open immediately, but remain closed for some time during that cycle. While the crack remains closed it is impossible to grow; crack growth is only possible during the ascending part of the stress cycle. The net effect of closure is to reduce the apparent ΔK to an effective level ΔK_{eff}.

$$\Delta K_{eff} = K_{max} - K_{open} \tag{13}$$

The stress intensity factor K_{open} in this equation is the minimum stress intensity level of that cycle to

re-open the crack, which is usually higher than the K_{min}. K_{open} is dependent on material thickness, R-ratio, K_{max} level, crack length, and environment. Using the concept of crack closure, Elber defined the effective stress intensity as follows:

$$\Delta K_{eff} = U \cdot \Delta K \tag{14}$$

[Ref. 2, 8]

where U is defined as:

$$U = \frac{K_{max} - K_{open}}{K_{max} - K_{min}} = \frac{1 - \frac{K_{open}}{K_{max}}}{1 - \frac{K_{min}}{K_{max}}} = \frac{1 - f}{1 - R} \tag{15}$$

With these last two equations, it is possible to rewrite equation 9 into the following equation:

$$\frac{da}{dN} = C(\Delta K_{eff})^n \frac{\left(1 - \frac{\Delta K_{th_{eff}}}{\Delta K_{eff}}\right)^p}{\left(1 - \frac{\Delta K_{eff}}{(1-f)K_c}\right)^q} \tag{16}$$

where $\Delta K_{th_{eff}}$ is defined as:

$$\Delta K_{th_{eff}} = \frac{1 - f}{1 - R} \Delta K_0 \left(\frac{4}{\pi} \tan{(1 - R)}\right) \sqrt{\frac{a}{a + a_0}} \tag{17}$$

The obtained crack growth equation (16) will be used to fit reported crack growth rate data. The main reason for presenting crack growth data K_{eff} versus da/dN is that the data can be written without the dependency of R, implying that only one set of constants in equation (16) can describe the behaviour of crack growth for different values of R. (See figure 13)

4.7 Finite element method to determine the stress intensity factor

Analytical solutions to problems in the mechanics of fracture are limited to idealised situations wherein:

- the domain is considered to be infinite,
- the material is homogeneous, and
- the boundary conditions are kept relatively simple.

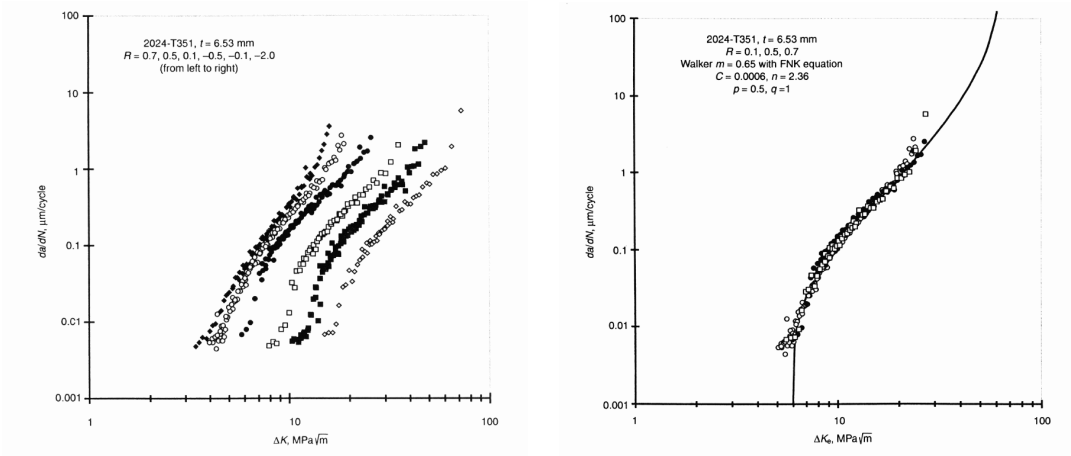

Fig. 13 Individual (left) and collective (right) data presentation

To deal with practical problems of mechanics of fracture in cracked structures of finite size, arbitrary shape, complicated boundary conditions, and arbitrary material properties, numerical methods as finite element methods (FEM) are necessary to produce actual stress intensity factor solutions.

Using the concepts of linear fracture mechanics to predict the strength and life of cracked structures, knowledge of the crack tip stress intensity factor as function of the applied load and geometry of the structure is necessary. Usually, standard models with standard stress intensity factor solutions are used to determine the stress intensity factor solution. In case of the 2^{nd}-stage fan disc a standard crack growth case could not be used because of the complicated geometry and a combination of multiple load cases. To determine the stress intensity factor as a function of the geometry, a finite element model will be used. The application of the finite element method allows analysis of complicated engineering geometries in two dimensional, and even three dimensional problems. The basic concept of the finite element method is that the structure can be considered to be an assemblage of individual elements. This is done by replacing the geometry of a structure by a finite amount of elements of finite size, which are connected through their nodal points. Known forces acting on these elements are transmitted through the nodal points, the displacements of the nodal points are the unknowns. In case of plane stress only two displacements, u and v, are used. These displacements are described with functions, e.g. assumed to vary linearly, or parabolically over the element.

In determining the stress intensity factor with finite elements, two different methods are available. The first, direct method, determines the SIF from the stress- or displacement field near the crack. The second, indirect method, determines the SIF through its relation with other quantities such as the compliance, the elastic energy, or the J integral.

In this case the direct method will be used to define the stress intensity factor. For fracture mode I, the stress and displacement distribution are given by :

$$\begin{aligned} \sigma_{ij} &= \frac{K_I}{\sqrt{2\pi r}} f_{ij}(\Theta) \\ u_i &= C K_I \sqrt{r} f_i(\Theta) \end{aligned} \tag{18}$$

K_I can be calculated from the stresses and the displacements respectively:

$$\begin{aligned} K_I &= \sigma_{ij} \frac{\sqrt{2\pi r}}{f_{ij}} \\ K_I &= \frac{u_i}{C\sqrt{r} f_i(\Theta)} \end{aligned} \tag{19}$$

Because finite element methods are usually formulated with displacements as the primary variables, displacements are computed more accurately than stresses, so better results are obtained using the lower equation of equation 19. [Ref. 10]

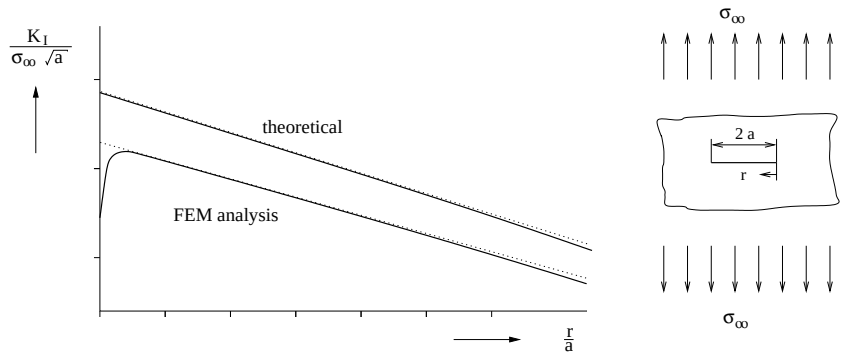

Fig. 14 FE and theoretical calculation of the SIF-solution for an infinite loaded plate with central crack

This last set of equations is valid in the immediate vicinity of the crack. The finite element method calculates the stress- and displacement distribution of the model. Using the stress and displacement of an element near the crack tip, obtained with FEM, values of K_I can be obtained by using the equation set 19. The stress intensity factor can be determined by extrapolating the constant slope, of a plotted $K/\sigma_\infty\sqrt{a}$ versus the distance r from the crack tip, back to the crack tip ($r = 0$). This is graphically shown in figure 14. [Ref. 11]

The reason that a difference exists between the theoretical (collocation techniques) curve and the FEM defined curve is that for this figure normal elements are used which do not take the effects of the stress singularity into account. Determining the K_I for several elements near the crack tip, a series of val-

ues for K_I are obtained. Using smaller elements will produce a more accurate solution, thus very small elements are needed. Even when using small elements, the determination of the SIF at very small distances from the crack tip is a little inaccurate due to the inability of the elements to represent the stress singularity at the crack tip. Accounting for the stress singularity is shown in appendix D. This appendix shows a derivation for an element which takes the effect of the stress singularity into account, which results in more accurate SIF solutions. Engineering fracture mechanics interest is often focussed on the singularity point, where quantities like stress become (mathematically, but not physically) infinite. Near such singularities normal, polynomial based, finite element approximations perform badly and attempts have frequently been made here to include special functions within an element which can model the analytically known singular function. An alternative to special functions within an element (which frequently poses problems of enforcing continuity requirements with adjacent, standard elements) lies in the use of special mapping techniques.

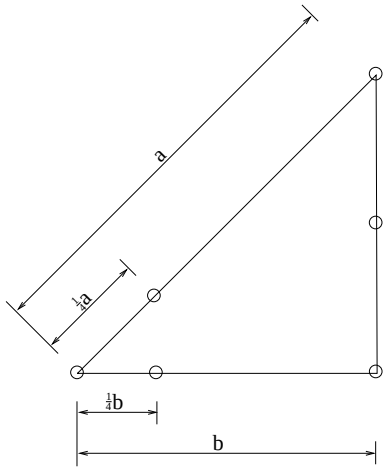

Fig. 15 Six node triangular finite crack tip element

An element of this kind was introduced by a simple shift of the mid-side nodes of quadrilateral, isoparametric elements to the quarter points. Although good results were achieved with such elements, the singularity is not well modelled on lines other than element edges. Better results are obtained by using triangular second-order elements for this purpose. (See figure 15) [Ref. 7, 11, 12, 13]

5 Research prior to life time calculation

To determine the propagation life of the 2^{nd}-stage fan disc, several aspects must be investigated. This includes the investigation of the load spectrum, the crack growth material properties, the stress intensity factor solution, and the stop criterion for the crack growth analysis.

5.1 Determination of the load spectrum

The life the aircraft components have is highly dependent on the weight of the missions. The initial mission usage (or design load) specification is very important for the success and use of the aircraft. If however, the actual mission usage of the engine deviates from the original concept, the risk of unacceptable failures increases. This brief introduction is given to emphisize the importance of engine load determination. Therefore loads acting on the rotating parts are to be recognised and determined. These loads consume life of the rotating parts, and must be accounted for in the life assessment. The most important loads on the rotating parts are:

- stresses due to bending moments, such as those due to the lift on the cascade airfoils or pressure differences across discs,
- torsional stresses are inevitable when power is transferred by shaft torque from turbines to compressors, and
- centrifugal forces are induced due to high rotational speeds.

The compressor fan disc is thus subjected to various types of loadings. As the air is propelled backwards, the compressor rotor blades tend to bend forward due to the resultant force acting on the blades. When this force is decomposed in axial and tangential direction, the axial force tends to pull the rotor blades in flight direction parallel to the longitudinal axis of the gas turbine shaft, and the tangential force causes a torsional moment in the LP shaft. Another load on the compressor blades is the radial force due to the high rotational speeds. The rotational speeds rise up to 14000 rpm, through which high centrifugal forces are inhibited. The radial forces have no influence on the crack growth analysis in the hub, because the forces on the rotor blades are balanced with the centrifugal force of the blades on the opposite side.

The axial forces can not be neglected because due the distance of the forces to the hub, a bending moment and an axial tension stress is introduced in the hub of the disc. This bending moment in the hub is believed to cause no stresses at all, due to the high torsion stiffness of the bore. Thus the stresses in the hub are the consequence of the axial force and the torsional moment.

5.1.1 Stresses due to axial force

Cracks are found during inspection intervals to develop from the air/thrust balance holes. If a cracked component is found the crack length will be reported, and the component will be rejected and replaced. It is believed at NLR that cracks grow under an angle of 45° with respect to the longitudinal axis of the gas turbine shaft, growing to the rear of the engine. Assuming this, the stresses due to the axial force must be much lower than the stresses due to torsional forces.

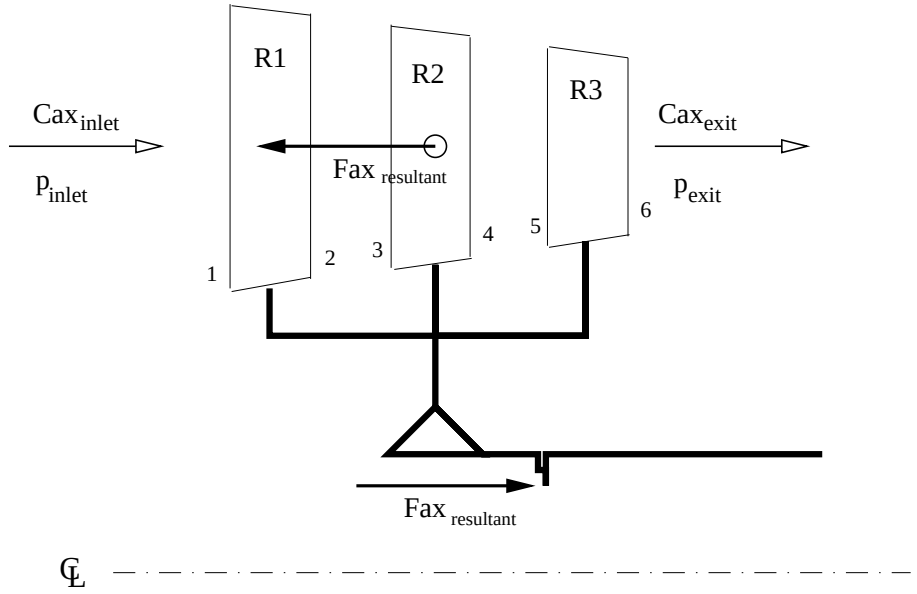

Fig. 16 Impulse balance

To confirm this assumption an impulse balance over the compressor (fan) is taken (see figure 16). The net axial force exerted on the fluid by each component is given by the streamwise increase in the quantity;

$$I = pA + \rho V^2 A \tag{20}$$

This equation is usually called the impulse function in one-dimensional gas dynamics. The streamwise axial force exerted by the internal solid surfaces of the component upon the fluid is $I_{exit\,rotor_i} - I_{inlet\,rotor_i}$ where i denotes the rotor number, while the axial reaction force is equal in magnitude, but opposite in direction. The net axial force includes all contributions of pressure and vicious stresses on

flow path walls and any bodies immersed in the stream.

$$\begin{aligned} F_{ax} &= I_{exit\,rotor_i} - I_{inlet\,rotor_i} \\ &= (p_2 A_2 + \rho_2 C_{ax_2}^2 A_2) - (p_1 A_1 + \rho_1 C_{ax_1}^2 A_1) \\ &+ (p_4 A_4 + \rho_4 C_{ax_4}^4 A_4) - (p_3 A_3 + \rho_3 C_{ax_3}^4 A_3) \\ &+ (p_6 A_6 + \rho_6 C_{ax_6}^6 A_6) - (p_5 A_5 + \rho_5 C_{ax_5}^6 A_5) \end{aligned} \tag{21}$$

The impulse function reveals the distribution of the major forces throughout the engine, but unfortunately does not precisely locate the distribution within the components. In case of a compressor or a turbine, forces can be *moved* from the rotor to the stator by means of static pressure forces applied to their extensions outside the flow path. These static pressure forces are often applied to circular discs and are therefore known as “balance piston” loads. (This explains the need of the thrust balance holes in the hub of the 2^{nd}-stage fan disc.) A strategy which is frequently employed is to manage the balance piston loads in such a way that most of the axial force is delivered to the stators, which are firmly attached to the outside casing of the gas turbine. This leaves only enough axial force on the shaft, which is attached to the rotors, to guarantee that the shaft thrust bearings, which prevents the axial motion of the shaft, always feels enough force to prevent the bearings from skidding, which rapidly consumes their life. This implies that the force exerted by the rotor is smaller than the value calculated with the impulse balance. [Ref. 14]

Solving the impulse function requires knowledge of many parameters as the inlet and outlet velocities (which are dependent on the angle of incidence), the static pressures at the inlet and outlet and the accompanying densities, and the geometry of the compressor disc and rotor blades. Many of these parameters are unknown. These parameters can be determined with extensive research, but that is beyond the scope of this project. To quantify the net axial force, an estimation will be made using the geometry of the compressor blade. The angle of the blade is observed to vary between $55°$ at the root of the blade, to an angle of $35°$ at the tip of the blade. The blade angle at mid-size is therefore $45°$. The assumption is made that the resultant axial force seizes at this point. With the known acting torque and the blade angle, the net axial force can be calculated to be equivalent to the tangential force (the tangential force is defined as the torque divided by the radius to the mid span). The obtained force is a conservative value, because the resultant force seizes at a distance larger than 50% of the blade height (usually approximately 70%), where the tangential force is smaller due to the increase in radius, and

the blade angle is less than 45° . [Ref. 15]

$$\begin{aligned} \sigma &= \frac{F_{tan}}{A_{hub}} \\ &= \frac{12 \cdot 10^3 / 0.35}{\frac{\pi}{4}(114.98^2 - 100.08^2)} = 13.6 MPa \end{aligned} \tag{22}$$

The steady state torque load at the design point is 12 kNm, resulting in a mean shear stress of 88.5 MPa. The magnitude of the axial stress is 15% of the value of the shear stress. The effect on the orientation in which the crack grows can be calculated with equation B.6 of appendix B. In appendix B the derivation of stresses to the principal stresses is shown.

Inserting $\sigma_x = 13.6\, MPa$, $\sigma_y = 0\, MPa$, and $\tau_{xy} = 88.5\, MPa$ in equation B.6 of appendix B shows that the influence of the axial force on the direction of the crack is observed to be minor. Due to the axial load the crack direction will be 42.8° with respect to the longitudinal axis in stead of 45° . To determine the influence of this change in growth direction due to the axial load, the life time is calculated (with use of CRAGRO) for two bi-axially loaded infinite plates. One of the plates is loaded with a σ_1 which is equal, but with reversed sign, to σ_2. The other plate is loaded with a σ_1 which is -0.857 times σ_2. The first plate is subjected to a maximum/minimum load of respectively 88.5 MPa and -88.5 MPa, while the second plate is subjected to a maximum/minimum load of respectively 95.57 MPa and -81.95 MPa. (These loads are determined by filling in equation B.7 of appendix B) Figure 17 shows the stress intensity factor solutions for both the load cases. This figure shows that the SIF solution of the case with the axial load is smaller than the case without the axial load. A conclusion which could easily be drawn from this figure is that the life-time of the axially loaded plate is bigger than the normally loaded plate, because the SIF appears to be smaller. This is in fact not true, because the vertical axis is scaled to the net stress. The stresses the axially loaded plate experiences are higher, resulting in a life time less than the case where the axial load is neglected. Two runs in CRAGRO are made. The result of the axially loaded plate is 88910 cycles for a crack to grow to 4.5 mm. For the other crack case, without the axial stress, a lifetime of 105010 cycles is obtained. The results of the life time calculations for these biaxially loaded infinite plates show that neglecting the axial component in the load spectrum results in an overestimation of approximately 18% from the plate where the axial force is not neglected. As noted earlier, a conservative approach is used, the actual percentage might be less.

This percentage is higher than anticipated in the first place, where the effect of the axial stress was neglected. The axial force is omitted in further calculations, but may produce a significant effect in the life time calculation. Therefore for further calculations the angle of crack growth is assumed to be

45°. [Ref. 14, 15]

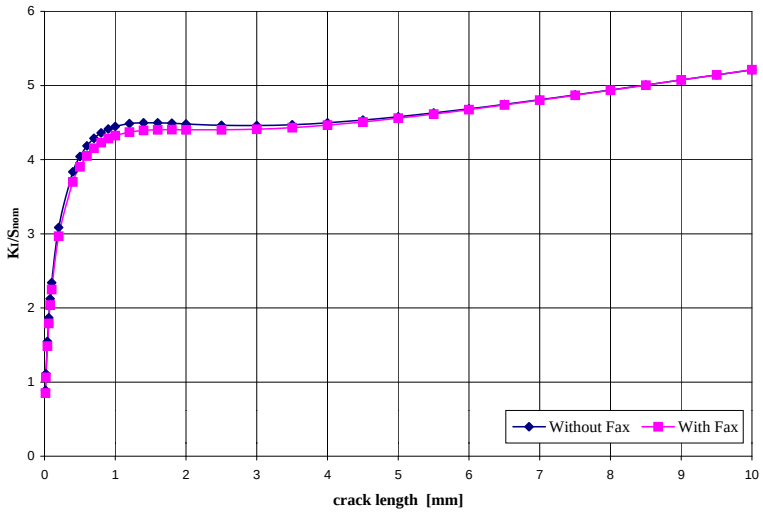

Fig. 17 SIF solution of two load cases

5.1.2 Stresses due to torsional effects

In the past years, NLR has build up expertise on gas turbine engine performance by supporting both military and civil aircraft operators as well as manufacturers with projects related to engine performance and handling, diagnostics, fuel consumption, health monitoring, etc. As an aid to predict, describe or analyse gas turbine behaviour, advanced modeling tools have been developed. NLR's main tool for gas turbine engine performance analysis is the *Gas turbine Simulation Program* (GSP). This program enables both steady-state and transient simulations of selected gas turbine configurations. An accurate model of the F-16 Pratt & Whitney gas turbine has been made at NLR, which will be used to determine the stresses in the compressor disc hub. To determine the stress in the disc due to torsion, the flight conditions and some engine parameters must be known. A system that measures the flight conditions and engine parameters several times per second is installed in the aircraft. The data is gathered by an acquisition system, called FACE, which is partly developed at NLR. This data acquisition system records for instance altitude, speed, free air temperature, rotational shaft speeds, turbine inlet temperature, exhaust nozzle area, and the fuel flows of the primary and core/duct augmentor (and many more if necessary). The data are imported in an Excel worksheet to be processed into a format usable for GSP. The variety in output data generated by GSP is wide, but for the load spectrum of the fan disc the torsional load on the fan shaft is needed. Fortunately all medium induced forces of the three sets of compressor blades will be transmitted through the 2^{nd}-stage fan disc. The 2^{nd}-stage fan disc transmits all loads of all three fan discs to the low pressure shaft through the hub.

The chosen torsional moment is not usable for crack growth programs, and must therefore be translated into (shear) stresses to be implemented in the load sequence. When a torque is applied to a uniform member with a circular cross section it tends to twist the member by rotating through an angle ϕ (angle of twist). During the twist all cross sections remain plain and undistorted (only for circular cross sections). The angle of twist is described by:

$$\frac{\tau}{r} = \frac{T}{J} = G\phi \tag{23}$$

The polar moment of inertia is described for a hollow shaft with inner diameter D_1 and outer diameter D_2 by:

$$J = \frac{\pi}{32}(D_2^4 - D_1^4) \tag{24}$$

To obtain a relation between the torque, the radii, and the shear stresses, equation 24 is substituted in equation 23. The shear stresses are proportional to the distance from the centerline, resulting in a maximum shear stress in the outer most fibre of the loaded member. (The geometry data of the hub is listed in table 2) (Figure 18 shows the shear stress distribution in a hollow shaft.)

$$\tau_2 = \frac{D_2 T}{\frac{\pi}{16}\left(D_2^4 - D_1^4\right)} = 7.8646 \cdot 10^{-6} \cdot T \tag{25}$$

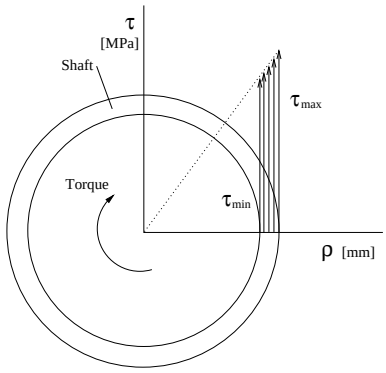

Fig. 18 Front view of a shear stress distribution in a torque loaded hollow shaft

This equation will be used to transform the torques, obtained with GSP, into shear stresses.

To calculate the torques, a GSP model of the Pratt & Whitney PW-F100-220 has been made at the helicopter department. With the data recorded by the FACE system as input parameters, the torque

Table 2 Fan disc geometry data

	Diameter [mm]	
D_1	100.08	[Inner]
D_2	114.98	[Outer]
Thickness	7.45	

in the LP shaft is calculated with a transient analysis. The results of the transient analyses of various missions are converted with an Excel based peak-valley program to obtain the local maximum and minimum values for several flight missions. The results of the transient analyses are stored in a database. Appendix C shows an overview of the various types of missions, which have been calculated with GSP.

From the mission database a loading sequence is made using the *mission mix* of the RNLAF. The mission mix presents the current distribution of the flown missions. Due to its confidential nature, because it reveals the training and defence strategy, this mission mix will not be explicitly stated in this report. Due to a lack of data for some of the missions, which are present in the mission mix, substitution with similar mission types (with respect to the severity) are conducted. With the use of a C++ based load sequence generator program, a random flight sequence of one thousand flights is generated. The code of the C++ program is listed in appendix G. The amount of the several missions, determined by the mission mix, is thereby taken into consideration. This sequence generator program produces a file which includes peak-valley shear stresses of one thousand flights. This file is the load sequence for the crack growth calculation.

5.2 Determination of the crack growth relation of Ti-6-2-4-6

The 2^{nd}-stage fan disc is made of a titanium alloy. The alloy is called Ti-6-2-4-6 or Ti-6Al-2Sn-4Zr-6Mo, where the numbers represent the amount of (wt%) alloying elements. In materials handbooks data points of the crack growth behaviour are tabulated. [Ref. 17] These data points are prepared with a macro based Excel sheet to be used in a commercial data-fit program which fits a curve (of prescribed form) through the data points. In the preparation Excel sheet, data points are converted from different units to SI units. See appendix H. Also the ΔK values are converted to ΔK_{eff}. This conversion enables the use of a fitting curve equivalent to equation 16;

$$\frac{da}{dN} = a(\Delta K_{eff})^b \frac{\left(1 - \frac{c}{\Delta K_{eff}}\right)^d}{\left(1 - \frac{\Delta K_{eff}}{e}\right)^f} \tag{26}$$

where,

$$
\begin{aligned}
a &= C \\
b &= n \\
c &= \Delta K_{th_{eff}} \\
d &= p \\
e &= (1-f)K_c \\
f &= q
\end{aligned}
$$

A difficulty in determining the fit parameters arises. The fit parameters c and e are assumed to be constant. In fact these fit parameters are not constant, but are dependent on the stress ratio R. Due to this dependence a loop (iteration) within the fit process is needed. (Because not all data points have the same stress ratio.) This loop and the small amount of datapoints make the fit process quite complex and thus instable, so no solutions are found for the fit parameters. For this reason fit parameters c and e are assumed to be constant, resulting in a marginal error in the fit solution.

However, the main difficulty in the fitting process is the absence of data points in the neighbourhood of the threshold value and the critical value. Therefore, often no convergence takes place in the fit proces solution procedure, or big inaccuracies occur. Due to the divergence, the threshold and critical value could not be obtained, and therefore values from the literature are used. Although the exact value is not known, the threshold is seen in the materials database of NASGRO to be of the same magnitude for various titanium alloys (a relatively small value is chosen to obtain a conservative calculation). The value of K_{Ic} on the other hand is not the same for most titanium alloys. K_{Ic} is the plain strain fracture toughness, which is a measure for the maximum crack resistance of a material. Due to the small diameter to thickness ratio in our case, the state of stress is plane stress. This means that deformations can easily occur and in that case the stress intensity factor depends on the plate thickness. The critical fracture toughness is dependent on the thickness of the specimen, and tends to increase for decreasing thickness. See figure 19. [Ref. 2, 7] This means that the K_c (the plain stress fracture toughness) is slightly higher than the K_{Ic} value. In this case the actual K_{Ic} from the materials handbook will be used. Because of the use of this value, crack growth calculations will be cut off sooner than expected, which implies that a conservative life time will be obtained. For the threshold value as in equation 17, the ΔK_0 = 69.5 $MPa\sqrt{mm}$, which will be used. The ΔK_0 in this equation is the ΔK at $R = 0$. For the plain strain fracture toughness an average value of 1340 $MPa\sqrt{mm}$ is used. [Ref. 17]

Because of these difficulties, two more methods are used to fit the data points. This is done with a simplified fit curve, which does not deal with the threshold and critical values. The simplified fit curve

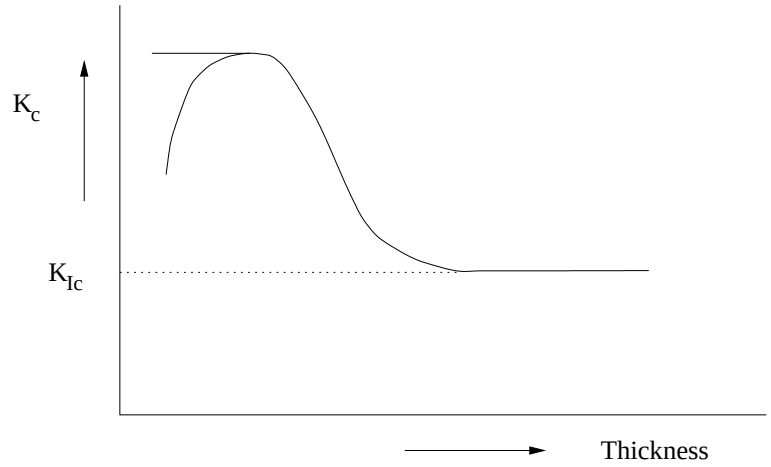

Fig. 19 The thickness effect on K_c

has the following form:

$$\frac{da}{dN} = a\,(\Delta K_{eff})^b \tag{27}$$

where,

a = C
b = n

This equation is used for both the commercial fit program as the trendline function within Excel. Figure 20 shows a fit of the Paris equation (equation 7) of the reported data points from ref. [Ref. 17] The fit parameters obtained with the three fit methods are tabulated in table 3. Table 3 shows

Table 3 Fit parameter overview of different fitting processes

Fit parameter		Method I Fit program	Method II Fit program	Method III Excel trendline
a	C	$1.35696 \cdot 10^{-10}$	$2.8109 \cdot 10^{-11}$	$7 \cdot 10^{-11}$
b	n	2.30657	2.5603649	2.4166
c	$\Delta K_{th_{eff}}$	$-2.68239 \cdot 10^{-5}$		
d	p	$6.0062 \cdot 10^{-3}$		
e	$(1-f)K_c$	1036.016		
f	q	$5.38343 \cdot 10^{-2}$		

that the various fit processes produce slightly different fit parameters. To describe the materials crack growth curve, C and n from all the three methods are taken from table 3, the K_{Ic} is taken from reference [Ref. 17], and the threshold value is taken from the NASGRO materials database (see page 45), which are to be used in the crack growth program.

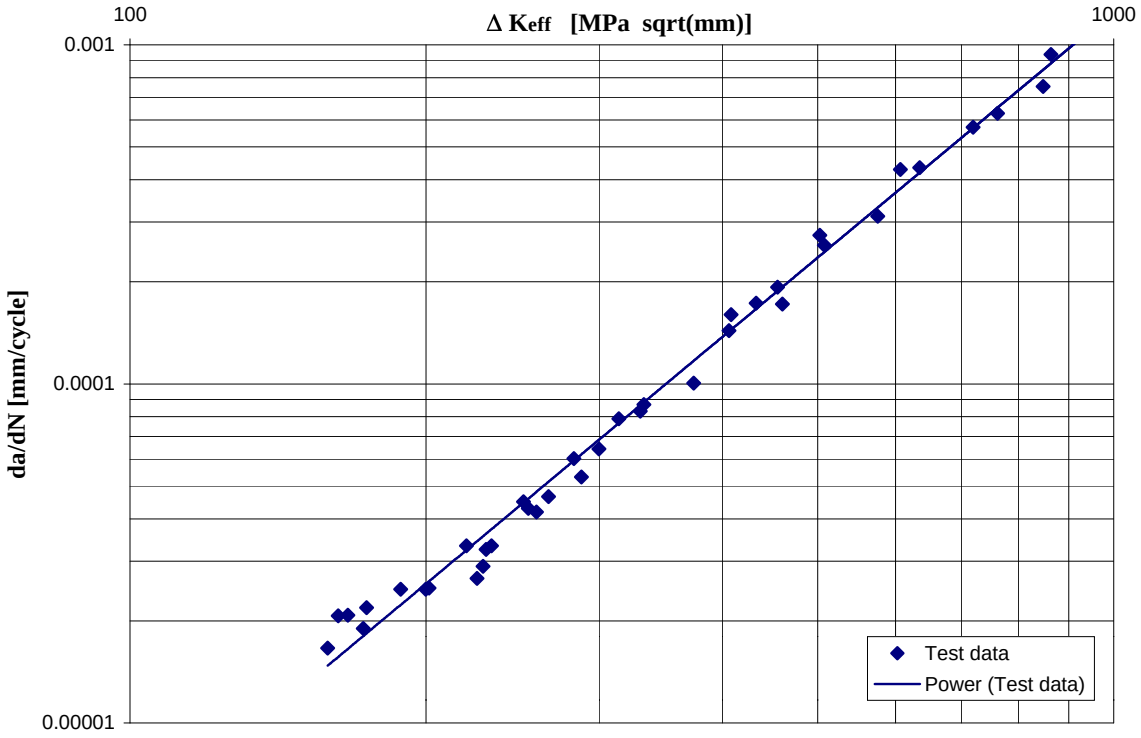

Fig. 20 Fitted crack growth data points

5.3 Determination of the SIF solution

To determine the stress intensity factor solution of the 2^{nd}-stage compressor fan disc, a finite element model is needed, because the geometry of the fan disc is too complex to use standard (infinite plate) SIF solutions. The fan disc is cyclic symmetric, and has 21 drilled air/thrust balance holes. The function of the air/thrust balance holes is to balance the pressure between the front and back side of the fan disc. [Ref. 17] Using the cyclic symmetric property in the FE model, only a small part ($\frac{1}{7}^{th}$) of the complete fan disc has to be modeled. Cracks are assumed to grow from the air/thrust balance holes under a 45° angle with respect to the axial direction, and will grow in the hub of the 2^{nd}-stage compressor fan disc. These cracks are considered *through the thickness cracks* so that the model can be constructed of two dimensional shell elements. For simplification reasons the whole model is constructed with the same shell thickness, because the hub has approximately the same thickness in

various sections. In the model the spacer/holder is not modeled, which will result in a conservative answer, because the crack growth rate will decrease due to the thicker section of the spacer/holder. The hub is connected to the disc, which is constructed of a relatively large piece of material called the bore, so that the model of the hub will be assumed to be supported. The boundary conditions are : $u_\theta = 0$, $u_z = 0$, $rot\, r = 0$, $rot\, \theta = 0$, $rot\, z = 0$. On the opposite side the load is applied at the middle of the spline as a distributed load on the shell elements. A graphical image of a FE model is shown in figure 21. This model is made for the stress intensity factor solution calculation of a 6 mm crack in the direction of the spline.

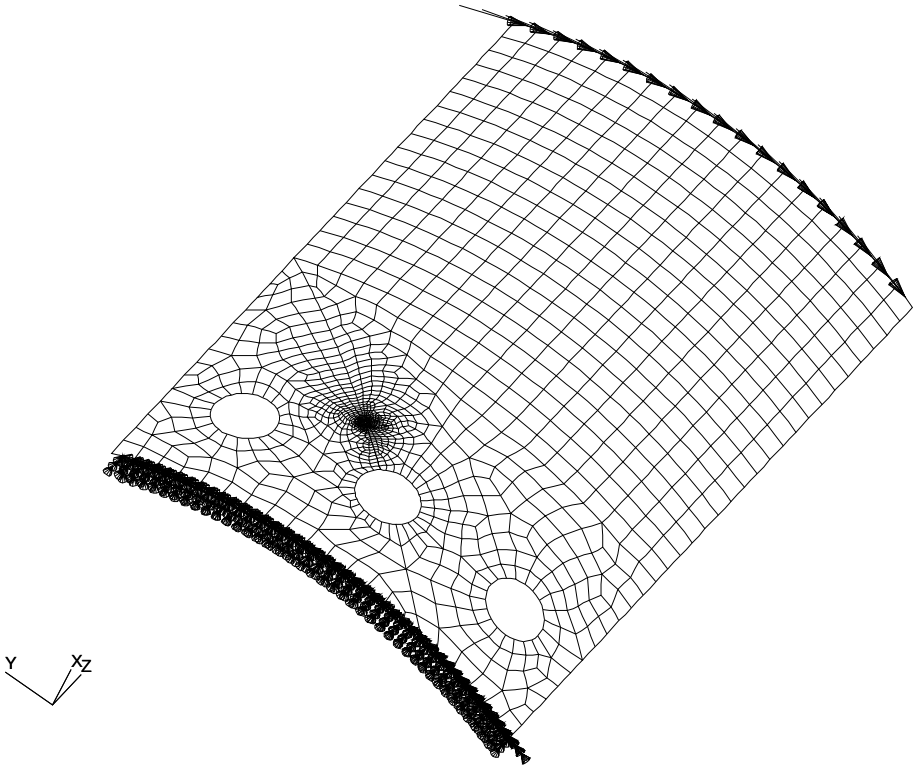

Fig. 21 Finite element model

Modeling the crack in the structure requires knowledge of the coordinates of the crack tip center on the surface. For that reason an Excel based program is written which calculates the coordinates as well as the length of the crack with respect to the origin of the crack. This is an important tool for constructing and meshing the model in a FEM program. The SIF solution is calculated with the use of PATRAN/NASTRAN. PATRAN is the pre- and post processor, which is used to create the geometry and the mesh. In the mesh at the cracktip in the surface of a square millimeter surrounding the cracktip, 4 elements are deleted. Of this model a data deck is generated for NASTRAN, the calculation program. Before running the data deck with NASTRAN, the data deck file is altered to

fit a special cracktip element in the mesh where the 4 elements have been deleted, because PATRAN does not support cracktip elements. This special NASTRAN cracktip element is called a CRAC2D element. Appendix I describes the use of this special crack tip element.

Figure 22 shows the deformed model, while figure 23 shows the first principal stress in the model.

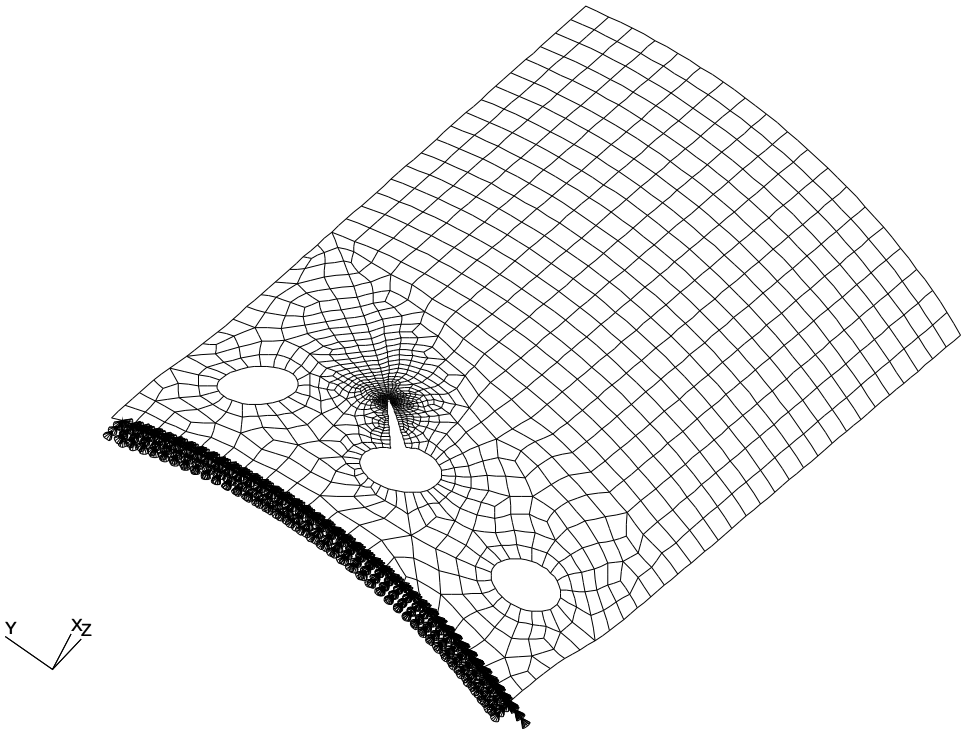

Fig. 22 Deformed finite element model

Several SIF solution calculations are performed for different crack sizes. These calculation are performed for a crack in the direction of the support and for a crack in the direction of the spline. The results of these calculations are graphically displayed in figure F.1 and figure F.2 of appendix F. Figure F.1 shows the results of the calculations compared to the results for a bi-axially loaded infinite plate with one hole. Figure F.2 shows even more stress intensity factor solutions for different loading types. Explanation of the legend is given in appendix F.

The figures clearly show that for large crack sizes, the SIF solution of the compressor fan disc approaches the solution of a bi-axially loaded infinite plate with a hole. For small crack sizes the influence of the thrust balance holes and the support is that large that the actual fan disc SIF solution deviates from the infinite solution. The actual SIF solution of the compressor fan disc will closely follow the path of the FEM calculated SIF solution, but will deviate when the crack approaches the

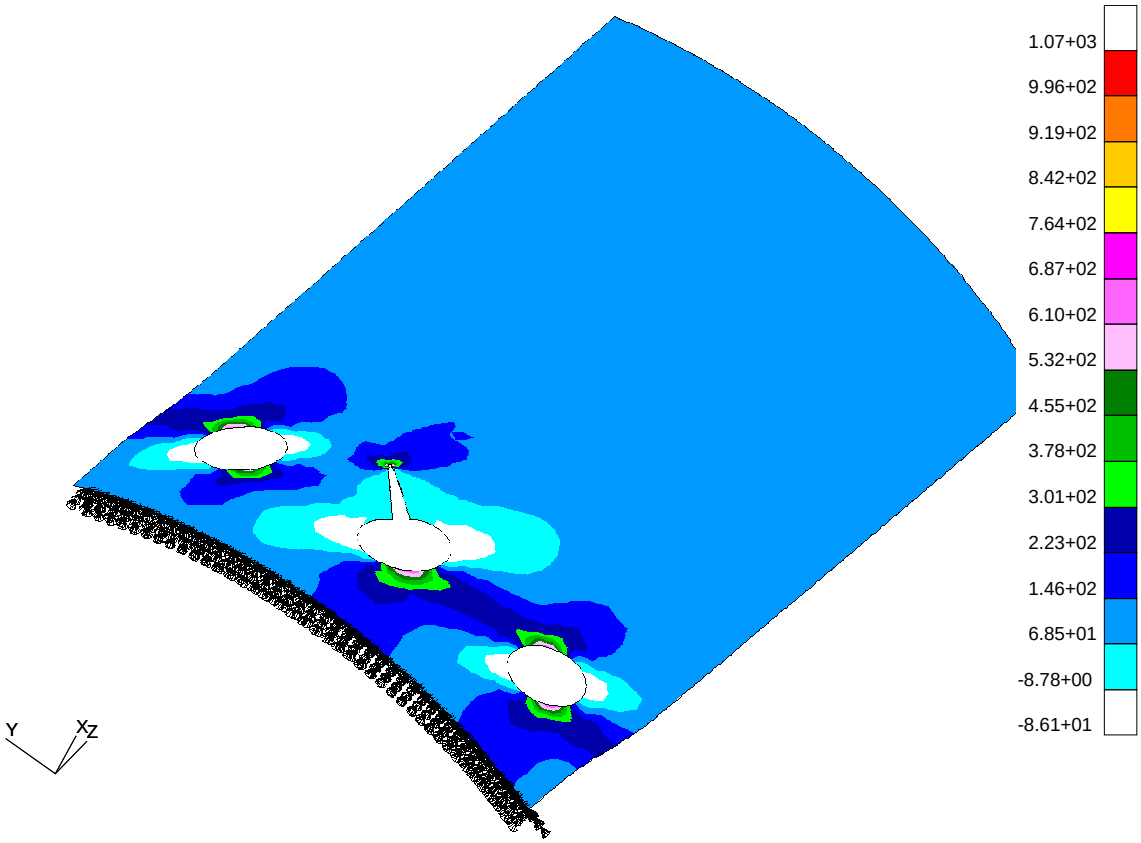

Fig. 23 Maximum principle stress in finite element model

length of approximately 4.5 mm due to the increase in thickness of the spacer/holder, which was not modeled.

5.4 Stop criteria for crack growth calculation

Failure or rejection of a component that contains a crack due to crack extension can be the result of three different causes.

- failure due to exceeding the plain strain fracture toughness K_{Ic},
- failure due to exceeding the net yield stress, or
- rejection due to technical or environmental issues (e.g. large cracks in fuel tanks will cause spilling of fuel, and therefore unacceptable)

Which one of the three stop criteria is applicable in case of the compressor fan disc calculation must be investigated prior to performing the crack growth calculation.

5.4.1 Exceeding the fracture toughness

From the load spectrum database the highest $\Delta\tau$ (shear stress) can be obtained. This is observed to be approximately 116 MPa. With the use of the stress intensity factor solution the ΔK *(max)* can be calculated. From the figures F.1, and F.2 one could imagine that the component will fail at the highest SIF. The local maximum SIF is reached at a crack length of 1.4 mm with a value of 5.68. This corresponds with a ΔK of 660 $MPa\sqrt{mm}$. The plain strain fracture toughness is assumed to be 1340 $MPa\sqrt{mm}$, which is higher than the local stress intensity factor, so the critical crack size is not reached at a crack length of 1.4 mm. To obtain an indication of the critical crack length, the biaxially loaded infinite plate with hole SIF solution and $\frac{K_{Ic}}{\Delta\sigma_1} = 11.55$ are used. This reveals (see figure 24) that the critical crack length will be much larger than 1.4 mm. The critical crack length exceeds the distance to the spacer/holder, so that the actual crack will stop growing or its crack growth rate will decrease. (The crack length to the spacer/holder is 5.5 mm)

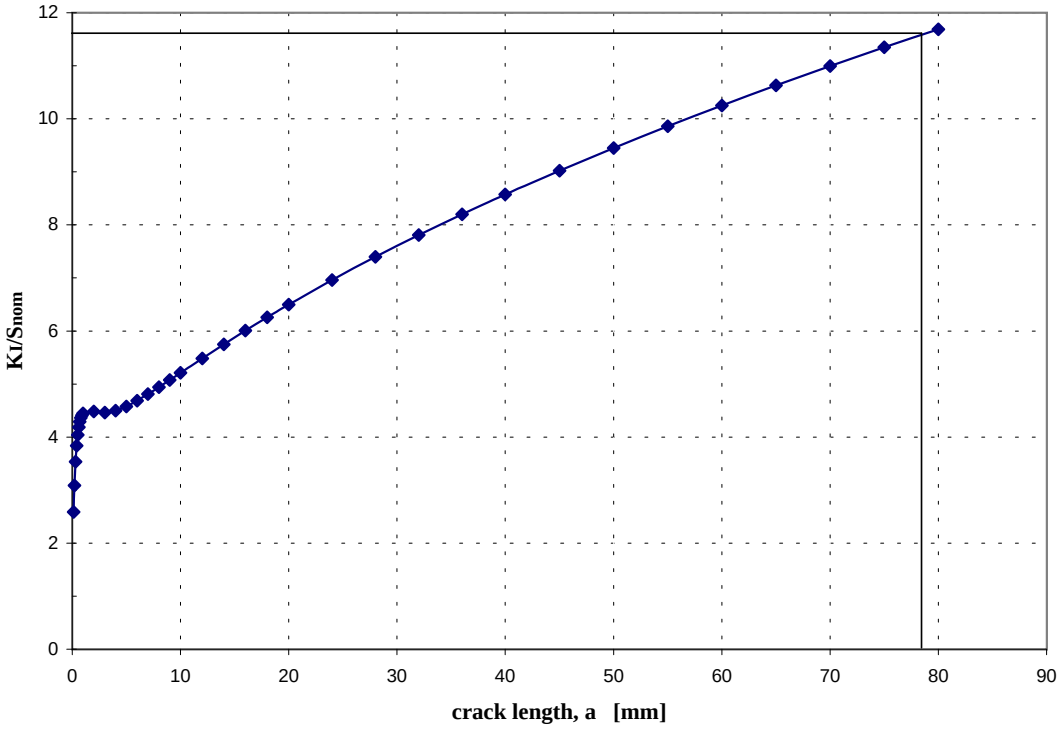

Fig. 24 Biaxially loaded infinite plate with hole

5.4.2 Exceeding the net yield stress

To determine the critical crack size at which the yield stress will be exceeded, an approximation of the compressor disc hub, a simple hollow cylinder, is used. The first principal stress (σ_1) tends to open the crack to 45° with respect to the axial direction. Along the surface of the cylinder an imaginary crack (l) can be assumed to be $\sqrt{2} \cdot hublength = \pm 141\, mm$. If a certain crack length is reached the net yield stress can be exceeded and the component will fail. This can be roughly estimated with:

$$\frac{\sigma_1 l}{l - (a - diam_{hole})} < \sigma_{yield} \tag{28}$$

$$\begin{aligned} \sigma_{yield} &= 1172 \quad \text{MPa} \\ \sigma_1 &= 125 \quad \text{MPa} \quad (\text{principal stress far from the support}) \end{aligned}$$

From which it follows that the crack can grow to a length of 120 mm before failure due to the exceeding of the net yield stress occurs.

5.4.3 Other rejection reasons

In aircraft wing structures components are rejected when cracks have extended to such lengths that fuel, oil, or hydraulic fluid cannot be contained in their designed compartment. In case of the hub it might be possible for cracks to grow to such rates that the the high pressure of the inner spool leaks to the outer spool.

5.5 Implementation

It is not likely for the crack to grow to rates specified in paragraph 5.4.1 or 5.4.2, because these values are very large they will result in large life times. Pratt & Whitney uses critical crack sizes which are substantially smaller than the crack sizes determined in paragraph 5.4.1 or 5.4.2, and must therefore have found a reason to assume small critical crack sizes. Therefore standard critical crack sizes from Pratt & Whitney are used. [Ref. 19]

The results of the above mentioned aspects will be used as input for the crack growth calculation program CRAGRO which will produce a crack based propagation life time. CRAGRO is a modular, stress intensity factor based, crack growth calculation program developed at NLR. This program is based on the NASGRO crack growth calculation program developed by NASA, but differs because of its modular design, which makes it relatively easy to expand the program with new equations or new models. Both programs lack the ability to take into account the contribution of creep and the influence of temperature. However, because the temperature in the fan disc is not very high, creep plays no role and can therefore be omitted in the calculation.

6 Crack growth calculation results

In the previous chapter all steps for the crack growth calculation are described. All these steps are incorporated in the crack growth program CRAGRO. The results will be presented and discussed in this chapter.

6.1 Results

As mentioned before the main object of this investigation is to determine whether the crack growth calculation could be made and secondly to determine whether the propagation life time of the 2^{nd}-stage fan disc is plausible. The propagation life time is the time in which an initial crack grows to the critical value. The propagation life is expressed in TAC's, which are the Total Accumulated Cycles. Each flight the RNLAF makes consumes a certain amount of cycles, expressed in the CCY number (Calculated CYcles). Dividing the TAC number by the CCY number the propagation life time of the 2^{nd}-stage fan disc is obtained in terms of flights. Due to the confident nature of the CCY number (because it reveals the RNLAF defence and training strategy) it will not be explicitly stated in this report. The CCY number seems to fluctuate over the years, because of its dependence on the type (mission mix) and the amount of flights. [Ref. 18] Therefore the propagation life time (determined by Pratt & Whitney Aircraft, PWA) is based on the lowest and the highest CCY number. The minimum life time according to PWA using appropriate CCY data of the past years is 2925 flights, while the maximum life time is 3382 flights.

The load sequence file contains 1000 flights. Because of this amount of flights, the crack growth calculation will be cut off in the middle of the file. CRAGRO reports in which line of the load sequence file the critical crack size or the fracture toughness is exceeded. Therefore a C++ program is written to determine in which flight the crack growth calculation is cut off. This program is called *Mission counter*. See appendix G for the code of that program.

The initial crack size used in CRAGRO is the crack size PWA uses for their calculations, the initial crack size (a_i) is 0.254 mm. Table 4 shows the results of crack growth calculations for the indicated critical crack lengths, using the initial crack size. PWA assumes different critical crack sizes for different parts of the component. The first column of table 4 shows typical values used by PWA for various parts in compressor discs. [Ref. 19] None of these parts correspond with our crack case, so that the calculated life times are not significant. The crack sizes are merely used for an indication of actual critical crack sizes.

Table 4 Overview of the CRAGRO results for various critical crack sizes

Critical crack size mm	Fit method I flights	Fit method II flights	Fit method III flights
1.6764	1062	1266	1130
2.3368	1523	1800	1602
2.7432	1822	2139	1912
2.8448	1887	2229	1993
3.1496	2124	2498	2234
4.2672	3025	3569	3195
4.7752	3467	4107	3663
4.8260	3513	4164	3711

6.2 Discussion of the results

Unfortunately the main disadvantage of the reported PWA propagation life time values is that it is not reported whether the component fails due to reaching the critical crack size, or that the component fails due to insufficient remaining strength, or is rejected due to another reason. Due to the unknown failure mechanism it is unknown when the crack growth calculation is cut off. Therefore, critical crack sizes of a 1^{st}-stage fandisc and a 2^{nd}-stage fan disc from the first design have been used.

The propagation life times of Pratt & Whitney can not exactly be compared with the calculated life times, due to the fact that the used critical crack sizes are not applicable for our used crack geometry. Most of the critical crack sizes in table 4 are taken from other locations than the hub, implying different load cases. The results however, show that the life times calculated with CRAGRO are of the same magnitude as the PWA life times. The results are slightly higher than the PWA results, because the effect of the axial force is not accounted for in the crack growth calculation, approximations in determining the crack growth relation, and inaccuracies in the SIF solution exist.

The results show that the design life time of the Pratt & Whitney calculations can be approximated assuming relatively short critical crack sizes of approximately 4.5 mm. Therefore Pratt & Whitney must have found a mechanism present in the component which adds to the normal loading, or Pratt & Whitney scaled their loading schedule with a safety factor. The loading sequence Pratt & Whitney uses to determine the propagation life of the 2^{nd}-stage fan disc is unknown and could well be scaled to account for problems such as augmentor instability. If the actual failure mechanism, or the severity of the Pratt & Whitney loading sequence is known, the propagation life time of the 2^{nd}-stage fan disc could be determined.

The 2^{nd}-stage fan disc of an USAF test engine failed prematurely (well before the propagation design limit). A confidential PWA report, [Ref. 20] , obtained from the RNLAF showed the premature failure to be due to combustion instability. Combustion instability induces pressure pulsations which produce torsional vibrations that excite the natural frequency of the disc. To determine the life of the prematurely cracked disc the torsional vibration loading must be added to the load sequence. The difference in propagation life time due to combustion instability in the augmentor is a result from idle to maximum augmentation. The combustion of fuel in the augmentor fuel nozzles produce pressure pulsations, which produce two effects. The first effect is that the pulsations are in direct contact with the fan-blades through the bypass (fan) duct. If the magnitude of these pulsations are big in relation to the size of the duct, all fan blades experience a change in angle of incidence, and therefore a change in the load magnitude and load direction. The second effect is that also the turbine rotor can contact the pressure pulsations causing the angle of incidence of the blades to alter. This effect results in torsinal vibrations and can excite the rotor in a torsional resonant mode. This extra load spectrum, which is not investigated, must be added to the normal loading sequence. This extra load spectrum consists of high frequency, low amplitude loads. These loads will lead to High Cycle Fatigue (HCF). HCF is of less importance for crack growth calculations because the life time can be expressed in minutes, so that the life of the component is strongly dependent on when the effect occurs. [Ref.15, 16, 20]

7 Conclusions and recommendations

7.1 Conclusions

- The life predictions, made by Pratt & Whitney, can be reproduced with CRAGRO, using realistic assumptions for the initial and critical crack length, even when the 20% error due to the axial compressor force is omitted in the load sequence. The path or stratagy followed is independent on the path followed by Pratt & Whitney.
- The performed crack growth calculations for the 2^{nd}-stage fan disc are in fact design calculations. This propagation life time is based on low cycle fatigue (LCF). If the mechanism for fracture or the severity index (safety factor) of the load sequence is known, the crack growth calculation indeed can be performed. This life limit differs from the actual life limit from the fractured test stand engine, because this fan disc is subjected to high cycle fatigue (HCF).
- Actual life predictions, for other components, can be performed when accurate material data, load sequence, stress intensity factor solution, and initial and critical crack lengths are known. A powerful tool in the determination of the stress intensity factor solution, is the use of finite elements. Usually infinite plate, or standard plate stress intensity factor solutions are used. These solutions are not applicable due to the high complexity of the component. This report shows that the two dimensional stress intensity factor solution for a real component can be calculated using FEM techniques.
- Due to large uncertainties in the determination of the fit parameters, uncertainties in the life time are obtained. To obtain a close fit for the crack growth calculation, many crack growth data is necessary, especially at the threshold and at the fracture toughness to define the asymptotes.

7.2 Recommendations

- To determine the stress intensity factor solution of a cracked component, many calculations for different crack lengths must be made. The geometry of the FE model differs slightly from one calculation to another. The main differences are the crack size and the mesh. The process of determining stress intensity factor calculations is time consuming, and could simply be computerised, so that the determination of the stress intensity factor solution could be speeded up.
- In this report the propagation design life time is determined for a component subjected to LCF. The actual test stand engine was also subjected to HCF. To account for HCF in the calculations, eigen frequency and computational fluid dynamic (CFD) calculations are needed. HCF life limits usually are very short, most of the times calculated in minutes. Therefore it should be considered if eigen frequency and CFD analyses are useful, if the excitation in the eigen frequency occurs failure is likely to follow very quickly. This could occur in the beginning or

at the end of the propagation life time. The actual life limit, including HCF, will be strongly dependent on when the excitation in the eigen frequency occurs.

- Most cracks start their life as corner cracks before they grow to *through the thickness* cracks. Hence a three dimensional stress intensity factor solution could be made and compared to the two dimensional stress intensity factor solution.
- Try to discover whether PWA has scaled their load sequence or what critical crack length they used to stop the calculation.
- Research on the extend of the axial compressor force by including the determination of the force within GSP using the impulse balance. Because this feature will not be used by most commercial GSP owners, the necessary data could be presented as output data, and processed in for instance an Excel sheet.

8 Discussion

The discussed thesis is presented and defended for an exam committee. The committee approved the thesis, but had some remarks.

FEM related remarks:

- One of the major concerns is that the FEM model is constructed as $\frac{1}{7}^{th}$ of the total hub, and constrained with cyclic symmetric constrains. This simplification is not quite correct, because this means the total hub would contain seven cracks. The effect of this representation would be that the model is less stiff than a model of the complete hub containing only one crack. This will yield a conservative answer. The problem with models of complete constructions is that the calculation time is much larger than for parts of those constructions.
- The load is introduced at half the distance of the spline. The spline would not permit the hub to rotate along the radial axis. This is not modeled, but again would this lead to a more stiff, consevative, model.

9 References

1. Grooteman, F.P.; *Fundamentals of Stochastic Analysis and Risk Assessment*, National Aerospace Laboratory NLR The Netherlands, February 1997, CR 97092 L.
2. Liu, A.F.; *Structural Life Assessment Method*, ASM International, first edition, 1998.
3. Cohen, H.; *Gas Turbine Theory*, Longman Group Limited, fourth edition, 1996.

4. United Technologies Pratt & Whitney; *F100 Fan Report*, United Technologies Pratt & Whitney, April 1990, FR-21278.
5. Tinga, T.; *Aerospace Lifing Methods, specifically for gas turbines*, National Aerospace Laboratory NLR The Netherlands, November 1998, CR 98511.
6. Kolkman, H.J.; *Discussion of the PWA lifing concept for the F100 engine -CIP task 463-*, National Aerospace Laboratory NLR The Netherlands, 1996, CR 96489 L.
7. Broek, D.; *Elementary Engineering Fracture Mechanics*, Sijthoff & Noordhoff, second edition, 1978.
8. *Fatigue Crack Growth Computer Program "NASGRO" version 3.00*, National Aeronautics and Space Administration, Lyndon B. Johnson Space Center, July 1996.
9. Newman Jr., J.C.; *A Crack Opening Stress Equation for Fatigue Crack Growth*, International Journal of Fracture, March 1984, Volume 24, R131-R135.
10. Fenner, R.T.; *Engineering Elasticity,Application of Numerical and Analytical Techniques*, Ellis Horwood Limited, first edition, 1986.
11. Chan, S.K.; et. al.; *On The Finite Element Method in Linear Fracture Mechanics*, Engineering Fracture Mechanics, 1970, Volume 2, pp. 1-17.
12. Atluri, S.N.; *Computational Methods for Plane Problems of Fracture*, Elsevier Science Publishers, Volume 2, 1986.
13. Zienkiewicz, O.C.; *The Finite Element Method*, mcGraw-Hill, fourth edition, 1994.
14. Mattingly, J.D.; Heiser, W.H.; Daley, D.H.; *Aircraft Engine Design*, AIAA Education Series, third edition, 1987.
15. Wolf, W.B. de; Verbal contact, National Aerospace Laboratory NLR The Netherlands, January 2000.
16. Visser, ir. W.; Verbal contact, National Aerospace Laboratory NLR The Netherlands, January 2000.
17. *Damage Tolerant Design Handbook*, Metals Ceramic Information Center, December 1993, Volume 24, Chapt. 4.
18. Heida, J.H.; Slauerhoff, J.F.; (Classified), *RNAF F100 Engine Usage Monitoring 1994-1997 (Confidential)*, National Aerospace Laboratory NLR The Netherlands, 1998, NLR-CR-99021.
19. Nethawa, D.H.; King, T.T.; *F100(3) Engine Structural Durability and Damage Tolerance Assessment Final Report*, Pratt & Whitney Aircraft Group, 6 June 1980, FR-10481-9.
20. Pratt & Whitney; (Classified); *Improved Durability 2^{nd}-stage fandisk (Safety Improvement)*, Pratt & Whitney, July 1996, Engineering Change Proposal (ECP) 94NA085.
21. Prof. dr. ir. L.J. Ernst; *College diktaat Sterkte en Stijfheid II*, Technische Universiteit Delft, Juni 1997.
22. Henshell, R.D.; *Crack Tip Finite Elements are Unnecessary*, International Journal for Numerical Methods in Engineering, 1975, Volume 9, pp495-pp507.

23. Newman, J.C.; *An Improved Method of Collocation for the Stress Analysis of Cracked Plates with Various Shaped Boundaries*, NASA, 1971, TN D-6376.

24. Rooke, D.P.; Cartwright, D.J.; *Compendium of Stress Intensity Factors*, The Hillingdon Press, first edition, 1976.

This page is intentionally left blank.

Appendix A Stresses and displacements at the crack tip

Irregularities such as holes, screw threads, and notches present in a member subjected to loading, may locally produce higher stresses than the remotely applied stress. This phenomenon is called stress concentration. The ratio of the true maximum stress to the stress that is calculated by ordinary formulas of mechanics using the net section (and ignore the changing in stress distribution), is the factor of concentration. For an infinite plate with a remotely applied uniform stress S, the theoretical stress concentration factor for an elliptical hole of semimajor axis a (on the x-axis) and end radius ρ is equal to:

$$K_t = 1 + 2 \cdot \sqrt{\frac{a}{\rho}} \tag{A.1}$$

or

$$K_t = 1 + 2 \cdot \frac{2a}{b} \tag{A.2}$$

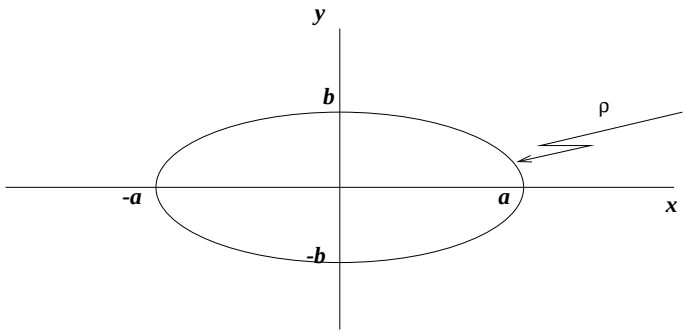

Fig. A.1 Elliptical crack

where b is the semiminor axis (on the y-axis). (See figure A.1) In case of a circular hole, if a equals b, the well-known stress concentration factor for a circular hole in an infinite sheet appears. $(K_t = 3)$ When b approaches zero, the ellips may be regarded as a crack. As a result the stress concentration factor becomes infinitely high. The local stress and displacement distributions near the crack tip, with coordinate system according to figure A.2, are given by:

$$\begin{aligned} \sigma_y &= \frac{K_I}{\sqrt{2\pi r}} \cos\frac{\Theta}{2}\left[1 + \sin\frac{\Theta}{2} sin\frac{3\Theta}{2}\right] \\ \sigma_x &= \frac{K_I}{\sqrt{2\pi r}} \cos\frac{\Theta}{2}\left[1 - \sin\frac{\Theta}{2} sin\frac{3\Theta}{2}\right] \\ \tau_{xy} &= \frac{K_I}{\sqrt{2\pi r}} \sin\frac{\Theta}{2} \cos\frac{\Theta}{2} \cos\frac{3\Theta}{2} \end{aligned} \tag{A.3}$$

For plane strain this becomes:

$$\begin{aligned} \sigma_z &= \nu(\sigma_x + \sigma_y) \\ \tau_{xz} &= \tau_{yz} = 0 \\ v &= \frac{K_I}{G}\sqrt{\frac{r}{2\pi}}\sin\frac{\Theta}{2}\left[2 - 2\nu - \cos^2\frac{\Theta}{2}\right] \\ u &= \frac{K_I}{G}\sqrt{\frac{r}{2\pi}}\cos\frac{\Theta}{2}\left[1 - 2\nu + \sin^2\frac{\Theta}{2}\right] \\ w &= 0 \end{aligned} \tag{A.4}$$

In these equations r is the absolute distance from the crack tip, v, u, and w the displacements corresponding to the directions of y, x, and z respectively. The constant G is the shear modulus of elasticity (or the modulus of rigidity), and is related to Young's modulus and Poisson's ratio by:

$$G = \frac{E}{2(1+\nu)} \tag{A.5}$$

For plane stress it yields:

$$\begin{aligned} \sigma_z &= \tau_{xz} = \tau_{yz} = 0 \\ v &= \frac{K_I}{G}\sqrt{\frac{r}{2\pi}}\sin\frac{\Theta}{2}\left[2 - 2\left(\frac{\nu}{1+\nu}\right) - \cos^2\frac{\Theta}{2}\right] \\ u &= \frac{K_I}{G}\sqrt{\frac{r}{2\pi}}\cos\frac{\Theta}{2}\left[1 - 2\left(\frac{\nu}{1+\nu}\right) + \sin^2\frac{\Theta}{2}\right] \\ w &= -\frac{K_I}{G}\frac{z}{\sqrt{2\pi r}}\left(\frac{\nu}{1+\nu}\right)\cos\frac{\Theta}{2} \end{aligned} \tag{A.6}$$

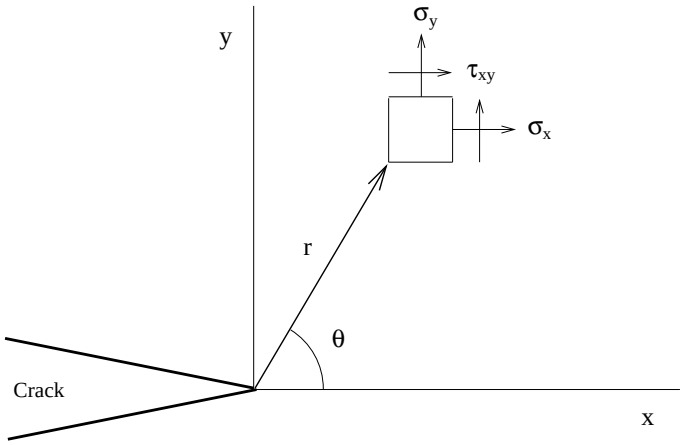

Fig. A.2 Coordinate system for stress/strain solutions

In these equations K_I is denoted as as the stress intensity factor, referring to the crack opening mode, which is the most common type of fracture. It should be emphasized that K is in no way related to plane stress or plane strain, because in either case the crack tip stress distributions are unchanged. The difference between the hypothetical plane stress and plane strain loci is not due to the stress components in the plane, because they are identical. Referring to A.3, K_I is not a function of the body, including the crack, i.e., crack size, geometry, location of the crack, and loading condition. The difference between plane stress and plane strain is hinged on the presence or absence of transverse constraint in material deformation in the vicinity of the crack tip.

In equations A.3, A.4, and A.6 some higher-order non-singular terms have been omitted. If r becomes rather small compared to planar dimensions, the magnitudes of the non-singular terms become negligible compared to the leading $1/\sqrt{r}$ term. Therefore, under ordinary circumstances inclusion of these terms is unnecessary.

[Ref. 2, 7]

Appendix B Derivation of principal stresses

The shear stresses due to the torque in the shaft can be transformed into principal stresses (without shear stresses) using the stress tensor. The reason for the translation into principal stresses is that the shear load case is not implemented in the crack growth program CRAGRO. Load cases such as bi-axially loadings are supported by the program. To obtain insigth in the magnitude of the principal stresses as result of the shear stresses the derivation of the principal stresses is given. The geometry of the 2^{nd}-stage fan disc is that complex that even the bi-axial load case is not suitable for the determination of the stress intensity factor solution, because this load case consists of an infinite plate with only one hole. Therefore will the stress intensity factor solution be constructed using the finite element method.

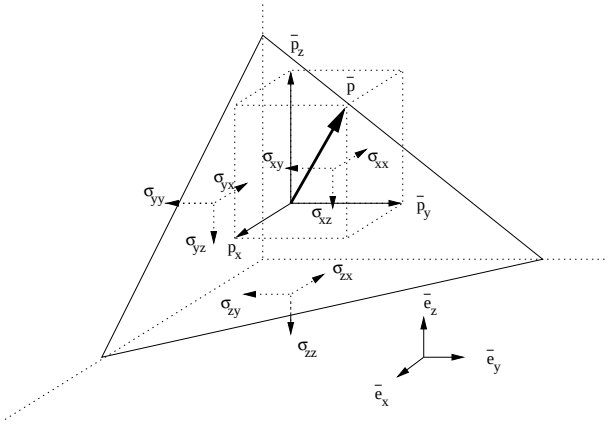

Fig. B.1 The stress vector

The shear stresses can be transformed into principal stresses with the use of a stress vector.21 Figure B.1 shows a vector perpendicular to a plane defined by its unit normal n. From equilibrium equations in the x, y, and z direction, it follows that:

$$\begin{bmatrix} p_x \\ p_y \\ p_z \end{bmatrix} = \begin{bmatrix} \sigma_{xx} & \sigma_{yx} & \sigma_{zx} \\ \sigma_{xy} & \sigma_{yy} & \sigma_{zy} \\ \sigma_{xz} & \sigma_{yz} & \sigma_{zz} \end{bmatrix} \cdot \begin{bmatrix} \widehat{n}_x \\ \widehat{n}_y \\ \widehat{n}_z \end{bmatrix} \tag{B.1}$$

This equation is usually written as:

$$\overrightarrow{p} = \Pi \, \overrightarrow{\widehat{n}} \tag{B.2}$$

In equation B.1 the σ-matrix is called the stress tensor (Π). This tensor appears to be symmetrical when moment equilibrium is considered of an infinitesimal part ($\Pi = \Pi^T$). This implies that the state of stress in point p is defined by six variables, i.e. three normal stresses and three shear stresses. In point p planes can be assigned where the shear stress component is equivalent to zero. In that case the stress vector coincides with the normal:

$$\vec{p} = \vec{\sigma} = \sigma \, \vec{\hat{n}} \tag{B.3}$$

which can be deduced to the following eigen value problem:

$$[\Pi - \sigma I] \cdot \vec{\hat{n}} = \vec{0} \tag{B.4}$$

The trivial solution is not usable, the non-trivial solution is found with:

$$det\,[\Pi - \sigma I] = 0 \tag{B.5}$$

This equation will produce three real valued roots, which are called the principal stresses of the point p.

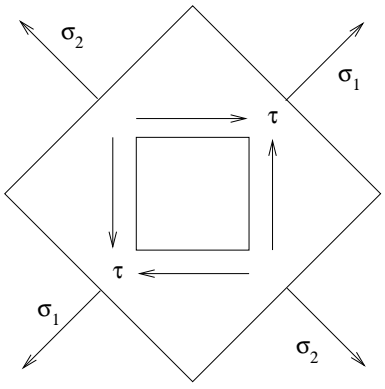

Fig. B.2 Visualization of principal stress transformation

Assuming plane stress due to small thickness to diameter ratio, terms σ_{xz}, σ_{yz}, σ_{zx}, σ_{yz}, and σ_{zz}

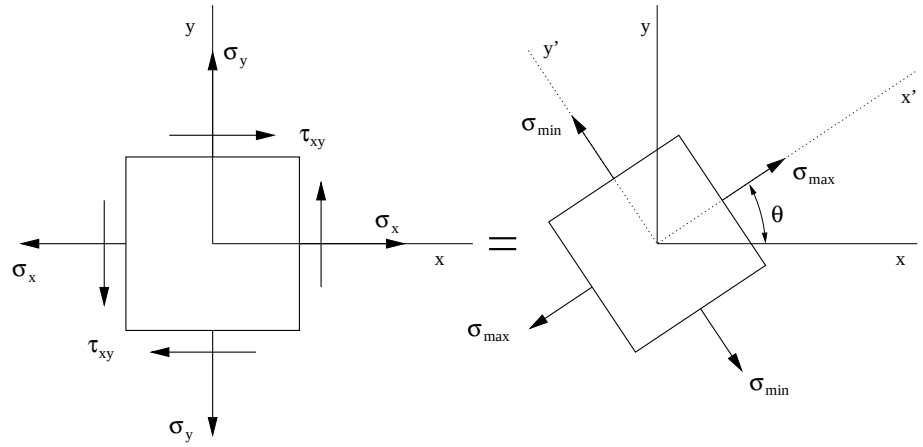

Fig. B.3 Transformation to principal stresses

reduce to zero. Using the eigenvalues (σ), the solution for this problem can be found with:

$$det \begin{bmatrix} \sigma_{xx} - \sigma & \sigma_{yx} & 0 \\ \sigma_{xy} & \sigma_{yy} - \sigma & 0 \\ 0 & 0 & -\sigma \end{bmatrix} = \mathbf{0}$$

Note that in case of the 2^{nd}-stage fan disc σ_{xx} and σ_{yy} are zero.

The solution (assuming $\sigma_{xy} = \sigma_{yx}$) of this problem reduces to $\sigma^2 = \sigma_{yx}^2$, which can be solved for σ_1 and σ_2. (Where σ_1 and σ_2 are the principal stresses.)

$$\begin{aligned} \sigma_1 &= \sigma_{xy} = \tau_{xy} \\ \sigma_2 &= -\sigma_{xy} = -\tau_{xy} \end{aligned}$$

The derivation shows that the normal stresses (which determine the crack growth direction) have the same magnitude as the shear stresses, but not the same direction (see figure B.2). Therefore a relation is needed which relates the applied torque to the shear stress in this specific case. The following will show a derivation which will relate the applied torque to the shear stress.

In case the stress condition is plane stress, with reference to figure B.3, the following equations can be deduced:

$$tan(2\Theta) = \frac{2\tau_{xy}}{\sigma_x - \sigma_y} \tag{B.6}$$

$$\sigma_{max,min} = \frac{\sigma_x + \sigma_y}{2} \pm \sqrt{\left(\frac{\sigma_x - \sigma_y}{2}\right)^2 + \tau_{xy}^2} \tag{B.7}$$

Appendix C Mission overview

Table C.1 shows an overview of the missions that are used for the crack growth calculation. Of these missions, sufficient data is recorded to perform transient analyses within GSP. The data is gathered by an acquisition system, called FACE. It records the fuel flow of both the combustion chamber and the flow of the afterburner, the nozzle area, and flight conditions (i.e. temperature, velocity, and pressure). These parameters are encorporated in a GSP model of the F100-PW-220 gas turbine. A graphical image of the GSP model of the F100-PW-220 is shown in figure C.1. With the input data, GSP calculates the torque in the Low pressure shaft, which can be transformed to shear stresses.

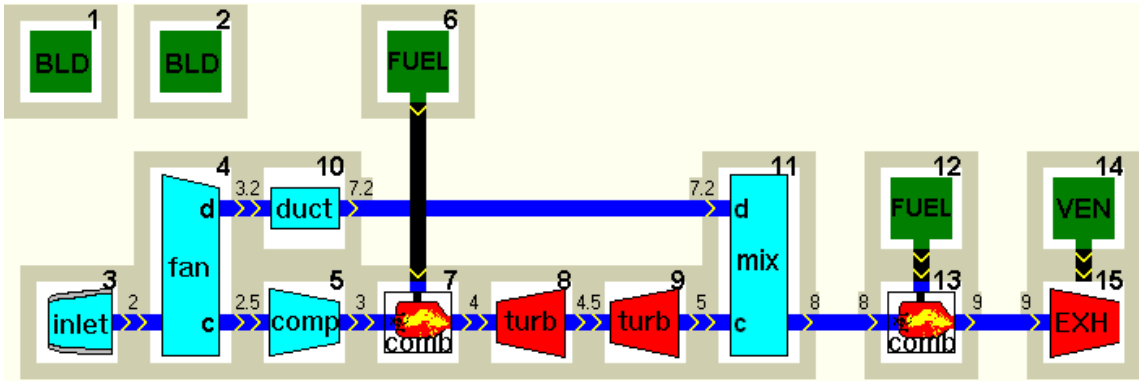

Fig. C.1 GSP model of the F100-PW-220

Table C.1 An overview of RNLAF missions

Flight number	Mission type	Flight number	Mission type
1	RECCE	11	ACT
2	RECCE	53	PI
3	RECCE	57	PI
4	RECCE	63	RANGE
5	ACT	65	AGNAV
6	ACT	66	RANGE
7	ACT	71	GF
8	ACT	77	AGNAV
9	RECCE	88	PI
10	ACT	99	RANGE

Appendix D Derivation of quarter side nodes for crack tip elements

Introduction

The finite element method is established as a standard tool for the detailed determination of stresses in engineering structures and components. Since the method is usually based upon assumptions for displacements and/or stresses, which are defined in terms of polynomial functions over elements of finite size, it is not possible to obtain exact representation of the behaviour in the region of a singularity. To overcome this difficulty the mesh near the crack tip, where the elastic stresses are singular, has to be substantially refined.

Local refinement of a mesh of standard finite elements in the region of the crack tip to reach sufficiently accurate values of stress intensity factors is usually found to be inpractical. Therefore, special crack tip elements have been developed, which in some cases merely involve relatively simple modifications to standard elements. [Ref. 22]

Crack tip elements

A simple approach for linear elastic problems involves modifications to the isoparametric elements in the neighbourhood of the crack. The purpose of these modifications is to impose the $\sqrt{r}$ stress and strain singularity which is known to exist near the tip of a crack in an elastic material , r being the distance from the tip.

The method of modification is only applicable to isoparametric elements employing polynomial shape functions of quadratic or higher elements. The required analysis can be conveniently outlined with reference to the simple line element shown in figure D.1.

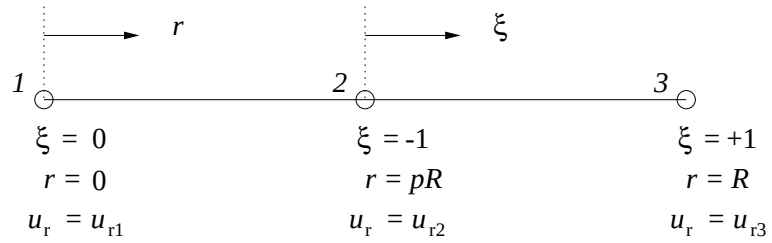

Fig. D.1 A quadratic line element

This line element can be regarded as one side of a general quadrilateral element. The physical distance, r, from node 1 and the displacement, u_r, in the r direction can be expressed as quadratic functions of the intrinsic coordinate, ξ, with equation D.1 and D.2.

$$r = \alpha_1 + \alpha_2\xi + \alpha_3\xi^2 \tag{D.1}$$

$$u_r = \beta_1 + \beta_2 \xi + \beta_3 \xi^2 \tag{D.2}$$

In these equations are α_i and β_i are constants defined in terms of nodal point values of r and u_r, respectively. Figure D.1 shows that, while $r = 0$ and $r = R$ at the first and third nodes, respectively, the second node where $\xi = 0$ is at $r = pR$, where the parameter p is as yet undefined. Substituting each of the three pairs of nodal points values of r and ξ in turn into equation D.1 leads to,

$$\begin{aligned} \alpha_1 &= pR \\ \alpha_2 &= \tfrac{R}{2} \\ \alpha_3 &= \tfrac{R}{2} - pR \end{aligned} \tag{D.3}$$

Substituting equation set D.3 into equation D.1 leads to,

$$r = R\left(p + \tfrac{1}{2}\xi + \left(\tfrac{1}{2} - p\right)\xi^2\right) \tag{D.4}$$

Differentiating this result with respect to ξ gives,

$$\frac{dr}{d\xi} = R\left(\tfrac{1}{2} + (1 - 2p)\,\xi\right) \tag{D.5}$$

The direct strain in the r direction is given by,

$$\epsilon_r = \frac{du_r}{dr} = \frac{du_r}{d\xi}\frac{d\xi}{dr} = \frac{du_r}{d\xi}\left(\tfrac{1}{2} + (1 - 2p)\,\xi\right)^{-1} \tag{D.6}$$

This equation is singular when $\frac{1}{2} + (1 - 2p)\,\xi$ equals zero. If $p = \frac{1}{2}$ as in unmodified isoparametric elements, this condition is never satisfied, and the strains remain non-singular. (If the same nodal points define the geometry and the finite element points; elements are considered isoparametric, i.e., the shape functions defining geometry and function are the same. [Ref. 13]) If, however, a singularity is required, for instance a crack tip at $r = 0$ and $\xi = -1$, then p has to be chosen to satisfy equation,

$$\tfrac{1}{2} - (1 - 2p)\,\xi = 0 \tag{D.7}$$

from which follows that $p = \frac{1}{4}$. In other words, the mid-side node in figure D.1 must be displaced to a point at quarter of the element length from the node at which the singularity is to occur.

Having created a singularity by shifting a node, it is appropriate to consider the order of the singularity. Setting $p = \frac{1}{4}$ in equation D.4 the following equation will be obtained:

$$r = R\left(\tfrac{1}{4} + \tfrac{1}{2}\xi + \tfrac{1}{4}\xi^2\right) \tag{D.8}$$

Solving this equation for ξ in terms of r and R will give:

$$\xi = -1 + 2\left(\frac{r}{R}\right)^{\frac{1}{2}} \tag{D.9}$$

Substituting this equation into equation D.2 for displacement,

$$u_r = \beta_1 + \beta_2\left(-1 + 2\left(\frac{r}{R}\right)^{\frac{1}{2}}\right) + \beta_3\left(-1 + 2\left(\frac{r}{R}\right)^{\frac{1}{2}}\right)^2 \tag{D.10}$$

from which may be obtained that the direct strain in the r direction is

$$\frac{du_r}{dr} = (\beta_2 - 2\beta_3)(rR)^{\frac{1}{2}} + \frac{4\beta_3}{R} \tag{D.11}$$

which, near $r = 0$, exhibits the $r^{\frac{1}{2}}$ singularity associated with the tip of a crack. [Ref. 10]

Appendix E Stress intensity factor calculation of a central cracked plate

To determine the density of the mesh in a finite element model, an analytically determined problem will be verified with a FEM model of a central cracked rectangular sheet with forces at the cracked centre. The example exists of a central cracked plate with outer dimensions 476 $\times$ 476 milimeter (mm) with a total crack of 238 mm. The layout of the plate is shown in figure E.1 and the dimensions in table E.1

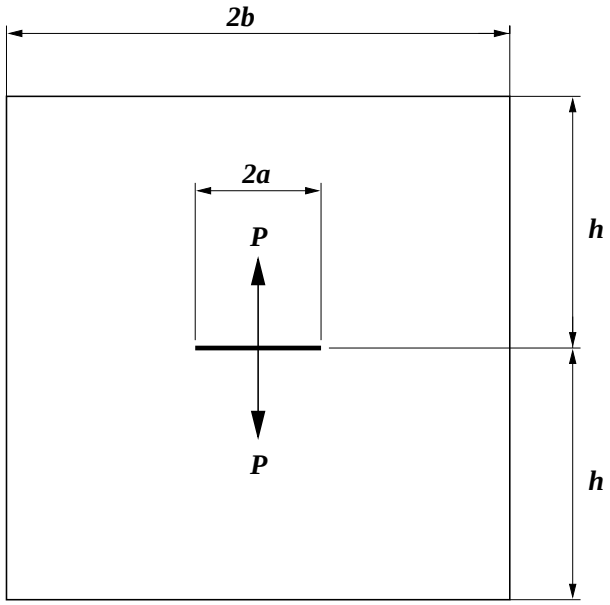

Fig. E.1 Geometry of the centre crack loaded plate

Table E.1 Values of plate geometry

item	symbol	value	unit
plate width	$2b$	476	mm
plate length	h	238	mm
crack length	a	119	mm
force at crack	P	2	N

Analytical approach using collocation techniques

A crack of length $2a$, subjected to forces per unit thickness P, acting at the centre of the crack surfaces, is located centrally in a rectangular sheet of heigth $2h$ and width $2b$ (see figure E.1). Newman 23has calculated (accuracy better than 1%) the opening mode stress intensity factor (K_I) for this configuration using collocation techniques. Boundary collocation is a numerical method used to evaluate the unknown coefficients in a series stress function. The method begins with a general series solution

to the governing linear partial equation (see equation E.1).

$$\begin{aligned} \nabla^4 \left(U\left(x,y\right)\right) &= 0 \\ \frac{\partial^4 U(x,y)}{\partial x^4} + 2\frac{\partial^4 U(x,y)}{\partial x^2 \partial y^2} + \frac{\partial^4 U(x,y)}{\partial y^4} &= 0 \end{aligned} \tag{E.1}$$

Wherein $U(x,y)$ is the Airy stress funcion. The biharmonic function $U(x,y)$ can be expressed as

$$U\left(x,y\right) = \frac{1}{2} Re\left[\int \overline{\Psi}(z)dz + \int \Phi(z)dz + (\overline{z} - z)\Phi(z))\right] \tag{E.2}$$

$$\begin{aligned} \sigma_x &= \frac{\partial^2 U(x,y)}{\partial y^2} \\ \sigma_x &= \frac{\partial^2 U(x,y)}{\partial x^2} \\ \tau_{xy} &= -\frac{\partial^2 U(x,y)}{\partial x \partial y} \end{aligned} \tag{E.3}$$

Certain terms are eliminated from the series by conditions of symmetry. The series is then truncated to a specific number of terms. The coefficients are determined through satisfaction of prescribed boundary conditions. The series solution obtained satisfies the governing equation in the interior of the region exactly and one or more of the boundary conditions approximately. Curves of K_I/K_0 versus a/b for various values of h/b are shown in figure E.2.

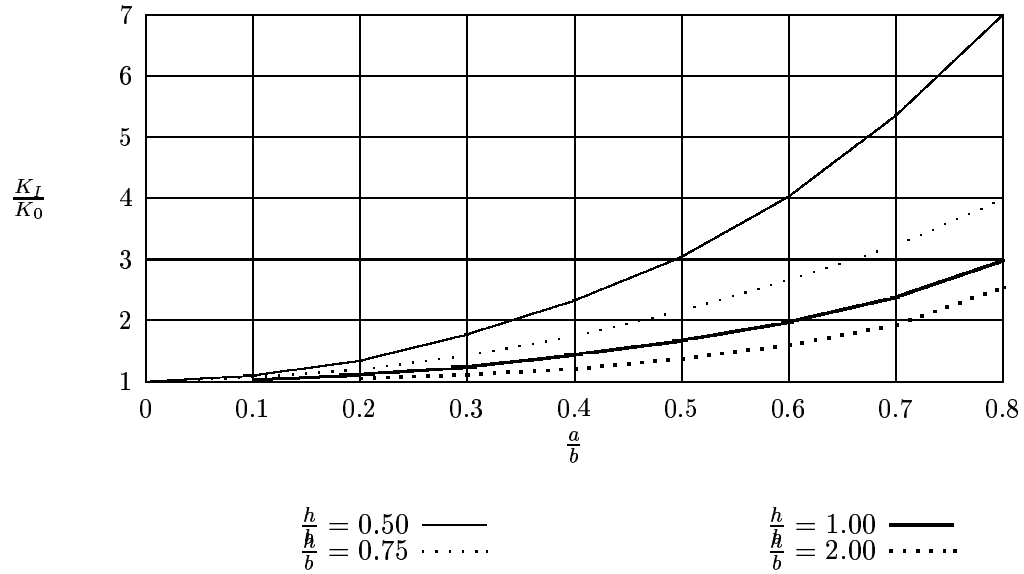

Fig. E.2 K_I for a central cracked rectangular sheet with opposing forces at the crack centre

Where K_0 is defined as the stress intensity factor for an isolated ($h = b = \infty$) crack subjected to centrally located opposing forces, P, is given by;

$$K_0 = \frac{P}{\sqrt{\pi a}} \tag{E.4}$$

The stress intensity factor of the sheet will be determined with the use of figure E.2, obtained from ref. 24. In the example $a/b = 0.5$ and $h/b = 1.0$ from which follows that $K_I/K_0 = 1.68$.

$$K_I = \frac{1.68 \cdot 2}{\sqrt{\pi a}} = 0.174 \tag{E.5}$$

FEM

For the calculation of the stress intensity factor a model of the central loaded cracked plate is necessary. Due to symmetry only a half of the plate can be modelled by using appropiate boundary conditions. The model is shown in figure E.3. Using the symmetry of the model, the boundray conditions for the section are:

$$\begin{aligned} u &= 0 \\ rot\, u &= 0 \\ rot\, w &= 0 \end{aligned}$$

All geometry data is taken from table E.1.

The stress intensity factor solution is calculated with NASTRAN for several mesh sizes (resp. 6, 12 and 24 elements over crack length), and with B2000 (for 6 elements over crack length). The solutions are presented in table E.2.

Table E.2 Results of FEM analysis

FEM program	elements over crack tip	K_I	error with respect to coll. techn.
NASTRAN	3	0.154852	$\pm 12\%$
NASTRAN	6	0.165799	$\pm 6\%$
NASTRAN	12	0.170161	$\pm 3\%$
B2000	3	0.170200	$\pm 3\%$

These results show that many elements are needed for NASTRAN, while B2000 only uses few to obtain solutions with the same deviation. For the calculation of the stress intensity factor solution of the compressor fan disc NASTRAN will be used due to the inability to use cilindrical coordi-

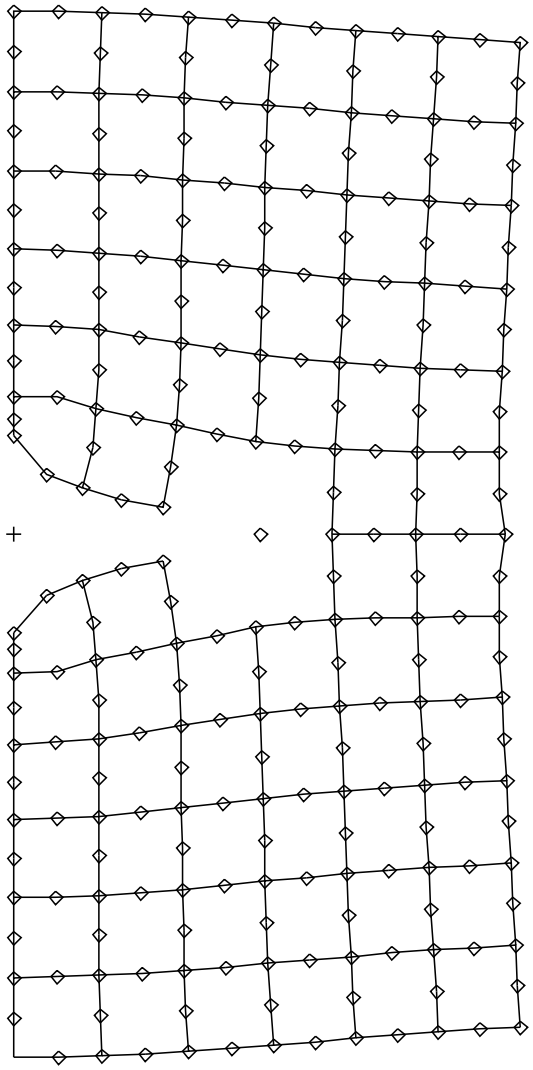

Fig. E.3 Finite Element Model of central loaded and cracked sheet

nate systems in B2000 which are necessary for the construction of the model and for the boundary conditions. Therefore special care must be taken in the determination of the mesh size within PATRAN/NASTRAN. The assumption is made that, *element size* = $\frac{1}{12}$· *crack size*, to obtain solutions with rather small deviation.

Appendix F FEM calculated stress intensity factor figures

In this appendix, two figures of the SIF solution are presented. The first figure (figure F.1) shows SIF's as a function of crack size, with the crack in the direction of the spline and with the crack in the direction of the support. For reference the NASGRO solution of a bi-axially infinite loaded plate with a hole is shown. The second figure (figure F.2) shows even more infinite plate solutions and has fitted curves through the FEM calculated SIF points.

In figure F.2 load cases TC09-bi refers to a bi-axially loaded infinite plate with one hole in the centre. Load case TC09-un presents the same plate but is uni-axially loaded. The TC03 load cases are uni-axially loaded plates with infinite length and finite width, with a hole in the centre. These infinite plate solutions are added to see the influence of the support and the holes in the FEM generated solution. For large cracks the SIF solution is seen to approach the TC09-bi load case, because the model of the hub is a cylinder with a uniform stress distribution.

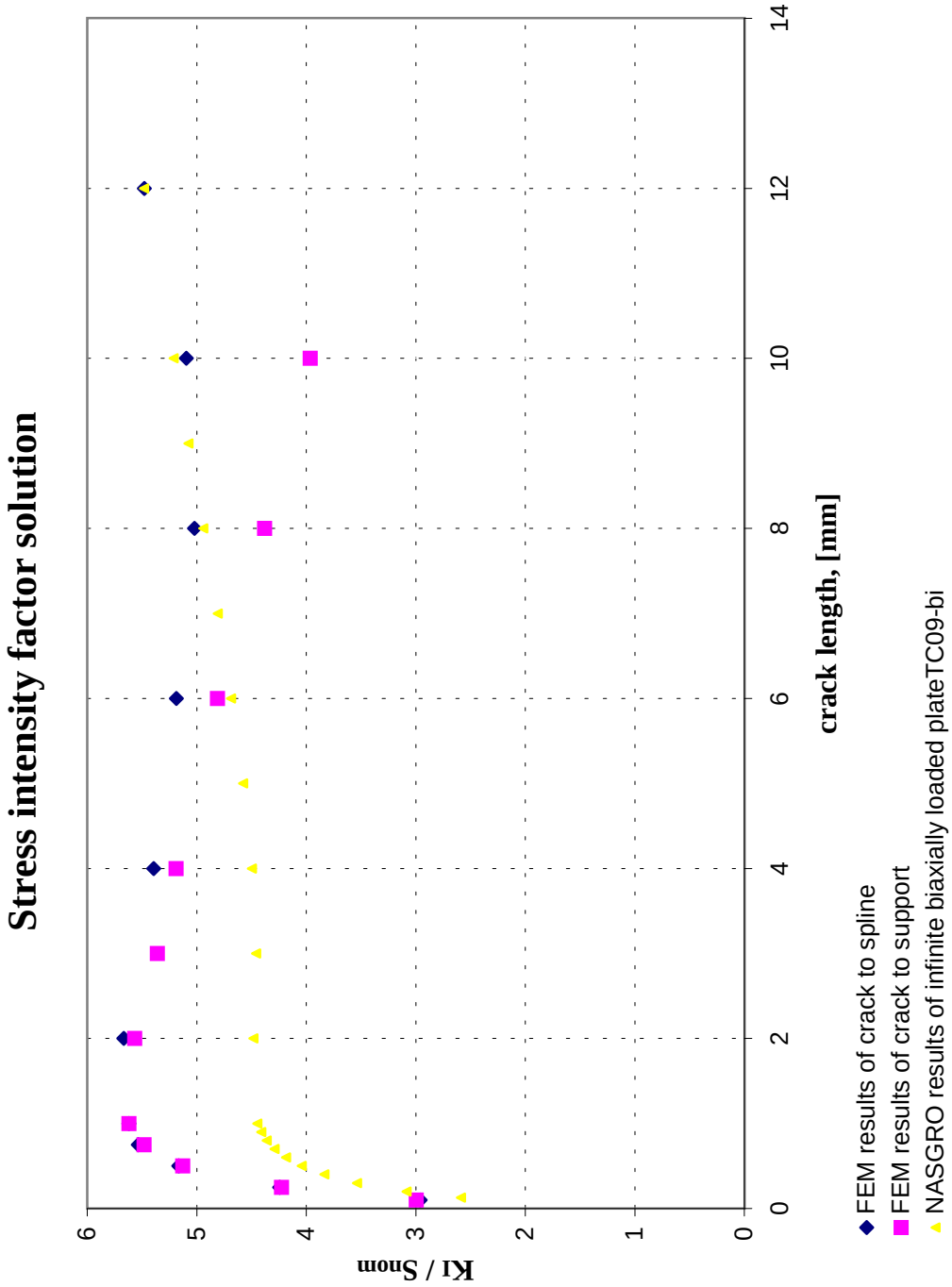

Fig. F.1 FEM calculated SIF

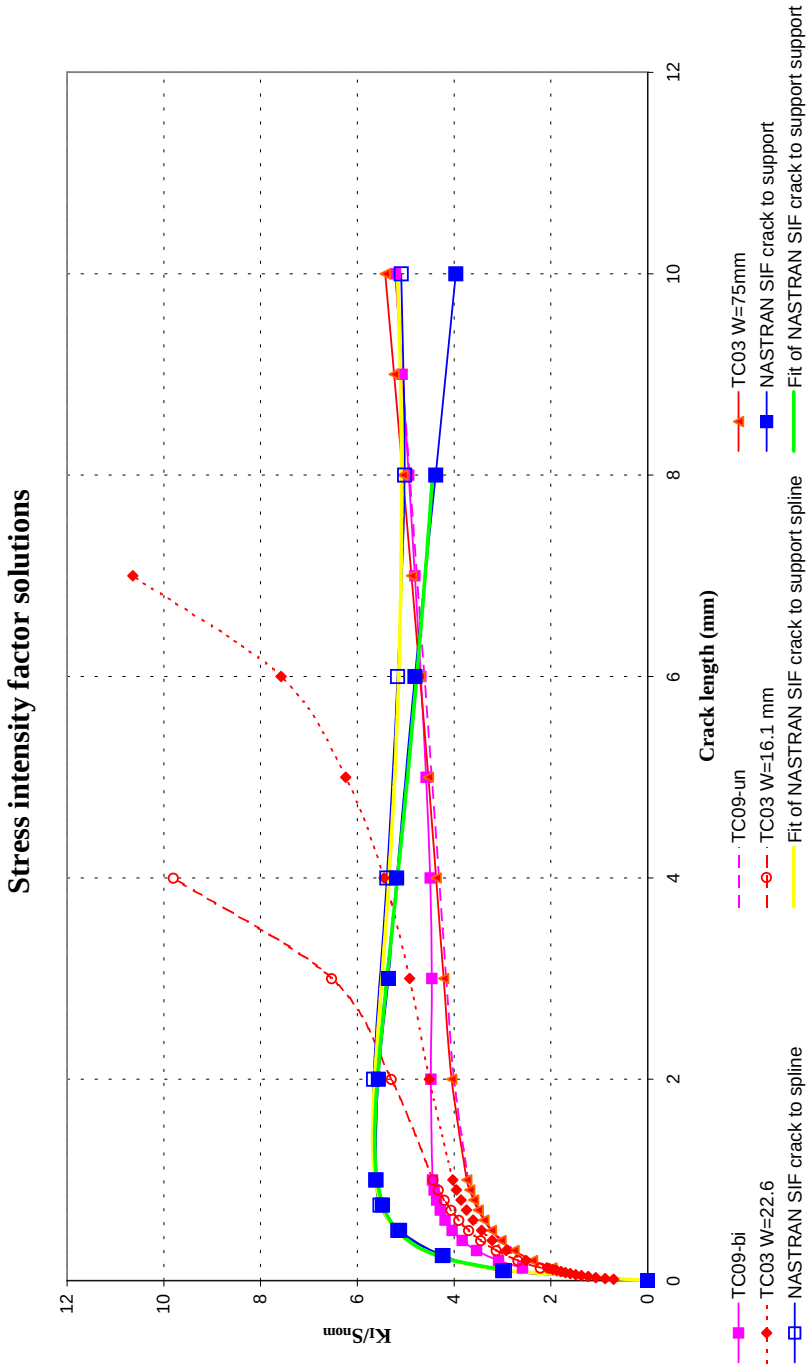

Fig. F.2 Fitted FEM calculated SIF

Appendix G C++ programs

In this appendix the C++ programs are listed that were developed for the crack growth calculation research. The first program listed is the load sequence generator, the second program is the mission counter.

Load sequence generator program

This program generates a random file of 1000 flights. To create the load sequence, data of the RNLAF mission mix is inserted in the program. The mission mix is classified, because it can reveal the defence and training stratagy. The mission mix values are substituted in the program by “XXX”.

```
#include <stdio.h>
#include <stdlib.h>
#include <iostream.h>
#include <new.h>
#include <limits.h>

int *initial(void);
int *teller(int waarde, int *tell);
int *shuffle(int *row);
int uitvoer(int *rij2, int *rij3);
int memory_error(size_t sz);
int *xpand(int *row2);

int main(void)
{
   int
    *rij, *rij2, *rij3;

   rij = new int [1000];
   rij2 = new int [1000];
   rij3 = new int [1000];

   rij = initial(); //maken van missie vluchten array
   rij2 = shuffle(rij); //door elkaar schudden van de missie array
   rij3 = xpand(rij2); //uitbreiden naar
```

```
                    //vluchten van een bepaalde missie

   uitvoer(rij2, rij3);

return(0);
}

int *initial(void)
{
   float
    recce=XXX, act=XXX, pi=XXX, gf=XXX, range=XXX, agnav=XXX;
// voor XXX relevante waarden invullen
   int
*row;

row = new int [1000];
  for (int i = 0; i < 1000; i++)
   {
    if (i < (recce*1000))
       row[i] = 1;
      if (i < (recce*1000+act*1000) && i >= (recce*1000))
       row[i] = 2;
      if (i < (recce*1000+act*1000+pi*1000)\
&& i >= (recce*1000+act*1000))
       row[i] = 3;
      if (i < (recce*1000+act*1000+pi*1000+gf*1000)\
&& i >= (recce*1000+act*1000+pi*1000))
       row[i] = 4;
      if (i < (recce*1000+act*1000+pi*1000+gf*1000+range*1000)\
&& i >= (recce*1000+act*1000+pi*1000+gf*1000))
       row[i] = 5;
      if (i < \
(recce*1000+act*1000+pi*1000+gf*1000+range*1000+agnav*1000)\
&& i >= (recce*1000+act*1000+pi*1000+gf*1000+range*1000))
       row[i] = 6;
    }
```

```
   return(row);
}

int *shuffle(int *row)
{
int
    *row2, i, j;

   row2 = new int [1000];

   j = (1000*rand())/RAND_MAX;
//hierdoor ontstaat een random getal tussen 0 en 1000
   for (i = 0; i < 1000; i++)
   {
      do j = (1000*rand())/RAND_MAX;
       while (row[j-1] == 0);
      row2[i] = row[j-1];
      row[j-1] = 0;
   }

return(row2);
}

int *xpand(int *row2)
{
   int
      k, nflights[6]={5,6,3,1,3,2}, *row3;

   row3 = new int [1000];  //hierin komen alleen de sub-vluchten

   for (k = 0; k < 1000; k++)
   {
      if (row2[k] == 1)
      {
        //random waarde genereren uit 5 vluchten
```

```
        row3[k] = (((nflights[0]-1)*rand())/RAND_MAX)+1;;
      }
      else
      {
        if (row2[k] == 2)
        {
           //random waarde genereren uit 6 vluchten
           row3[k] = (((nflights[1]-1)*rand())/RAND_MAX)+1;
        }
        else
        {
           if (row2[k] == 3)
           {
        //random waarde genereren uit 3 vluchten
              row3[k] = (((nflights[2]-1)*rand())\
/RAND_MAX)+1;
           }
           else
           {
              if (row2[k] == 4)
              {
        //random waarde genereren uit 1 vlucht
                 row3[k] = (((nflights[3]-1)*rand())\
/RAND_MAX)+1;
              }
              else
              {
                 if (row2[k] == 5)
                 {
        //random waarde genereren uit 3 vluchten
                    row3[k] = (((nflights[4]-1)*rand())\
/RAND_MAX)+1;
                 }
                 else
                 {
                    if (row2[k] == 6)
```

```
                    {
       //random waarde genereren uit 2 vluchten
                     row3[k] = (((nflights[5]-1)*rand())\
/RAND_MAX)+1;
                    }
                    else
                    {
                    printf("Flight number does not exists\n");
                    }

                 }

              }

           }

        }

      }
   }
return(row3);
}

int uitvoer(int *row2, int *row3)
{
   int
    l, i, num, p, q, *tell, *tell2;
   int
        telarr[6] = {0,0,0,0,0,0};

   int
      vluchtmatrix[6][6] ={{ 0, 1, 2, 3, 4,-1},
                           { 5, 6, 7, 8, 9,10},
                           {11,12,13,-1,-1,-1},
                           {14,-1,-1,-1,-1,-1},
                           {15,16,17,-1,-1,-1},
```

```
                    {18,19,-1,-1,-1,-1}};
char
 *getal, **fname;


FILE
   *infile[20], *outfile;

   tell  = new int [6];
   tell2 = new int [6];
   getal = new char [15];
   fname = new char* [6];

   tell = telarr;

   fname[ 0] = "F001.txt"; //RECCE 1
   fname[ 1] = "F002.txt"; //RECCE 2
   fname[ 2] = "F003.txt"; //RECCE 3
   fname[ 3] = "F004.txt"; //RECCE 4
   fname[ 4] = "F009.txt"; //RECCE 5

   fname[ 5] = "F005.txt"; //ACT 1
   fname[ 6] = "F006.txt"; //ACT 2
   fname[ 7] = "F007.txt"; //ACT 3
   fname[ 8] = "F008.txt"; //ACT 4
   fname[ 9] = "F010.txt"; //ACT 5
   fname[10] = "F011.txt"; //ACT 6

   fname[11] = "F053.txt"; //PI  1
   fname[12] = "F057.txt"; //PI  2
   fname[13] = "F088.txt"; //PI  3

   fname[14] = "F071.txt"; //GF  1

   fname[15] = "F063.txt"; //RANGE 1
   fname[16] = "F066.txt"; //RANGE 2
```

```
      fname[17] = "F099.txt"; //RANGE 3

      fname[18] = "F065.txt"; //AGNAV 1
      fname[19] = "F077.txt"; //AGNAV 2

   for (p = 0; p < 6; p++)
   {
      for (q = 0; q < 6; q++)
      {
        if (vluchtmatrix[p][q] != -1)
        {
           num = vluchtmatrix[p][q];
           if (!(infile[num] = fopen (fname[num], "r")))
           {
              cout << "Kan Flight" << (i+1)\
<< ".txt niet openen\n";
              exit(1);
           }
        }
      }
   }

   if (!(outfile = fopen ("result.txt", "a")))
   {
      cout << "Kan result.txt niet openen\n";
      exit(1);
   }

// voor elk cijfer n in row2 goede file kopieren naar outfile:
   for (i = 0; i < 1000; i++)
   {
      p = row2[i]-1;
      tell2 = teller(p+1, tell);
      tell = tell2;
      q = row3[i]-1;
      num = vluchtmatrix[p][q];
```

```
      printf("row2,row3,file = %d,%d,%s\n",row2[i],row3[i]\
,fname[num]);
      fprintf(outfile, "%s", "0\n");
//    kopieren van een inputfile naar outfile :
      fseek(infile[num], 0, 0);
      while (fscanf(infile[num], "%s", getal) != EOF)
      {
        if (fprintf(outfile, "%s", getal) == EOF)
           cout << "Foutje bij schrijven naar outfile";
        fprintf(outfile, "%s", "\n");
      }
   }

   //nu nog een 0 toevoegen na laatste file
   fprintf(outfile, "%s", "0\n");

   for (l = 0; l < 20; l++)
   {
      fclose(infile[l]);
   }

   fclose(outfile);

   cout << "\nAantal 1:" << tell[0];
   cout << "\nAantal 2:" << tell[1];
   cout << "\nAantal 3:" << tell[2];
   cout << "\nAantal 4:" << tell[3];
   cout << "\nAantal 5:" << tell[4];
   cout << "\nAantal 6:" << tell[5];

   return(0);
}

int *teller(int waarde, int *tell)
{
switch ( waarde )
```

```
{
case 1 :
   {
    tell[0] += 1;
      break;
   }
case 2 :
   {
    tell[1] += 1;
      break;
   }
case 3 :
   {
    tell[2] += 1;
      break;
   }
case 4 :
   {
    tell[3] += 1;
      break;
   }
case 5 :
   {
    tell[4] += 1;
      break;
   }
case 6 :
   {
    tell[5] += 1;
      break;
   }

 default :
   {
    cout << "Geen 1, 2, 3, ,5 of 6 !!\n";
      break;
```

```
      }
}
return(tell);
}
```

Mission counter

To determine in which one of the thousand flights the crack growth calculation is cut off, the following program is used. The input of this program is the line number where the crack growth calculation has stopped, which is reported by the crack growth calculation program. The output is the number of passed flights and the flight number where the calculation is cut off.

```
#include <stdio.h>
#include <stdlib.h>
#include <iostream.h>
#include <new.h>
#include <limits.h>

int main(void)
{
   int
      zoekregel, vluchtteller, regelteller;
   int
      con_ok;
   float
      *getal;
   char
      *fname;
   FILE
      *infile;

   getal=new float [15];
   fname="result.sf";
   if (!(infile = fopen (fname, "r")))
   {
      printf("Kan %s niet openen !!!\n", fname);
```

```
      exit(1);
   }

//read first value of result.sf
   fseek(infile,0,0);

   regelteller = 1;
   vluchtteller = 0;
   printf("Enter het regelnummer waar CRAGRO berekening de ");
   printf("maximale scheurlengte overschreed.\n");
   con_ok=scanf("%d",&zoekregel);

      if (con_ok != 1)
        printf("mislukt geen 1 integers gelezen");
   printf("Regel waarop gezocht wordt = %d\n",zoekregel);

   while ((fscanf(infile,"%f",getal) != EOF)\
&& (zoekregel != regelteller))
   {
//      printf("getal = %f\n",getal);
      if (*getal == 0)
      {
       vluchtteller = vluchtteller + 1;
        printf("regel = %d\n",regelteller);
        printf("vlucht = %d\n",vluchtteller);
      }
      regelteller = regelteller + 1;
   }

   fclose(infile);

//uitvoer
   printf("Invoer regelnummer        = %d\n",zoekregel);
   printf("Gestopt bij regelnummer   = %d\n",regelteller);
   printf("Aantal doorlopen vluchten = %d\n",vluchtteller-1);
   printf("Gestopt in vlucht         = %d\n",vluchtteller);
```

```
   return(0);
}
```

Appendix H Fitting crack growth data

To produce the fit for the materials crack growth curve, a Microsoft Excel sheet is written which processes crack growth data to a form usable for a commercial datafit program. (Instructions are given on the first data sheet of the Excel program) The items the user has to enter are: materials crack growth data points and common data, which units are used. When these data are entered, a macro must be activated, which will process the data into a form usable for the datafit program. When this macro has completed the converted data can be copied to the commercial datafit program. To obtain the fit first a general equation must be generated to which the data must be fitted. Such an equation has the following form:

$$\frac{da}{dN} = a(\Delta K_{eff})^b \frac{\left(1 - \frac{c}{\Delta K_{eff}}\right)^d}{\left(1 - \frac{\Delta K_{eff}}{e}\right)^f} \tag{H.1}$$

Where $\frac{da}{dN}$ equals Y and ΔK_{eff} equals X, and the letters a through z represent the fit constants. This equation is just an example, other, more complex equations are possible (taking e.g. the stress ratio and the crack opnening function into account).

Appendix I Implementation of CRAC2D elements in NASTRAN input files

Introduction

When engineering fracture mechanics, finite element models are frequently used to calculate stress intensity factors. The finite element program NASTRAN of the MacNeal-Schwendler corporation is capable to produce stress intensity factors because special cracktip elements are programmed. To use the special cracktip elements, PATRAN (the pre- and post processor) cannot be used, because it does not support cracktip elements. To implement these special cracktip elements in cracked finite element models, the bulk data deck (this is a file containing the code of the model) has to be altered. Difficulties were encountered using the cracktip elements. Therefore a description of the use of the special cracktip elements is added to this report.

Applying CRAC2D elements

To use CRAC2D elements in a model, some details have to be considered. First, when building the geometry of the model in a pre-processor like PATRAN, special interest must be taken in the vicinity of the tip of the crack. When building the geometry, a square surface of approximately 1 cm^2 must be modelled with the centre of the square as the tip of the crack. Brake this surface with a modelled crack, so that two rectangels are obtained. Mesh these surfaces to obtain square elements (four- or eigth node elements), using an even mesh seed on the long side of the rectangle (e.g. 10) and half of the long side mesh seed for the short side of the rectangle (e.g. 5). Delete the four elements surrounding the tip of the crack, without deleting the nodes. With the EQUIVALENCE option, all double nodes (not for the crack) must be deleted. With the option SHOW, the outer node numbers and the centre (cracktip) node of the 4 deleted elements must be obtained and reported on paper. Using four node elements, 10 nodes must be reported (**G1** through **G10**). Using eight node elements, 18 nodes must be reported (**G1** through **G18**). See figure I.1 This ends the work in the pre-prossor, so make a NASTRAN analysis deck of the model to obtain the bulk data deck file (*filename.bdf*).

From the NASTRAN analysis deck (*filename.bdf*) some key elements have to be added to produce the analysis deck with the crack tip elements. These are:

- ADUMi element, defines attributes of the dummy element;
- PRAC2D, defines properties of the crack tip element;
- CRAC2D, defines two-dimensional crack tip element.

§ **ADUMi**

This element is called a dummy element. This dummy element contains information about the amount

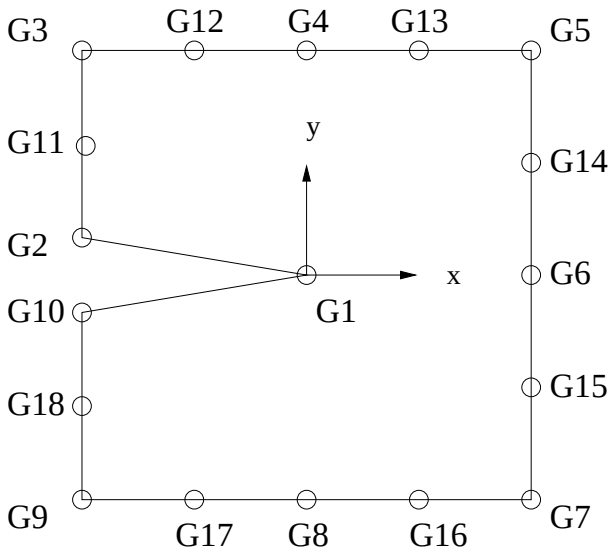

Fig. I.1 NASTRAN cracktip element

of grid points of the cracktip element, and the number of additional fields for other entries. The format of this element is shown in table I.1. Fill in this element the total number of nodes usually 18 or 10, and the name of the element type (in this case CRAC2D).

ADUMi	NG	NC	NP	ND	ELNM	-	-	-	-

NG	Number of grid point connected by DUMi element
NC	Number of add. fields on CDUM connection entry
NP	Number of add. fields on the PDUMi prop. entry
ND	Number of displacement compo. at each grid point
ELNM	Name of element connection

Table I.1 Format ADUMi

§ **PRAC2D**

This command is used to define the element properties of the cracktip element. The format of this command is shown in table I.2. This command is used to give the cracktip element a specific thickness, wich must be equivalent to the thickness of the shells surrounding the cracktip element. With the IPLANE option it is possible to define the state of stress. Use 0 for plane strain; 1 for plane stress. Use for the GAMMA and the PHI option the default value, because non-default values are not tested by NASTRAN yet.

§ **CRAC2D**

PRAC2D	PID	MID	T	IPLANE	NSM	GAMMA	PHI	-	-

PID	Property id number of PRAC2D entry
MID	Material id number
T	Thickness
IPLANE	Plain stress/strain option
NSM	Non-Structural Mass per unit area Default=0
GAMMA	Default=0.5
PHI	Default=180.0

Table I.2 Format PRAC2D

This command is used to define the cracktip element. The format of this element is shown in table I.3. The reported node numbers from PATRAN correspond with G1 through G18 in the CRAC2D command.

CRAC2D	EID	PID	G1	G2	G3	G4	G5	G6	
	G7	G8	G9	G10	G11	G12	G13	G14	
	G15	G16	G17	G18					

EID	Element id number
PID	Property id number of PRAC2D entry
Gi	Grid point id number

Table I.3 Format CRAC2D

The description of the 3 command are necessary to use cracktip elements in a finite element model. The following lines are taken from a from a bulk data deck file of a cracked hub.

```
ADUM8    18   0    5    0    CRAC2D
PRAC2D   999  1    7.45 1    0    0.50 180.
CRAC2D   1322 999  1128 1236 1268 1266 1264 1111 +   ZZZ1
+   ZZZ1 1113 1130 1147 1145 1251 1267 1265 1249 +   ZZZ2
+   ZZZ2 1112 1123 1140 1146
```

In this case the element number is 1322 with material properties 999. A plane stress analysis will be carried out on an element with a thickness of 7.45 mm. The ADUM8 element specifies 18 nodes, which are filled in the CRAC2D command (beginning with 1128 ... ending with 1146). Note that the node numbers correspond with the right $\mathbf{G_i}$ numbers. The $+$ $\mathrm{ZZZ_i}$ statements are used because one

line may not contain more than 10 arguments. Using this statement, the program knows more data will folllow one the next line with the same + ZZZ_i.

Output

If the above procedure is followed a NASTRAN analysis can be run. This will produce several files. The most important file is the file called *filename.f06*. Open this file in a text editor and search for the CDUM element. This will yield an output with the format according to table I.4. The SIF for mode I can be found on position S6.

S1	S2	S3	S4	S5	S6	S7	S8	S9
x	y	σ_x	σ_y	τ_{xy}	K_I	K_{II}	0	0

Table I.4 Format CDUMi output

Typical output lines, taken from a f06 file from a cracked hub model, are:

```
         S T R E S S E S   I N   U S E R   E L E M E N T S (CDUM8)

EL-ID  S1      S2      S3      S4      S5       ....
1322   4.9E-02 6.8E-06 7.8E+02 1.2E+03 -7.5E+01 ....

      .... S6       S7      S8     S9
      .... 6.4E+02 -5.2E+01 0.0    0.0
```